



Recent Progress on Blue Quantum Dot Light-Emitting Diodes from Materials to Device Engineering

Youngwoo Jeon¹ · Hyungsuk Ryu¹ · Hyunho Lee¹

Received: 29 April 2024 / Revised: 19 June 2024 / Accepted: 9 July 2024

© The Author(s), under exclusive licence to Korean Institute of Chemical Engineers, Seoul, Korea 2024

Abstract

Quantum dots (QDs) are gaining widespread attention for their applications as light-emitting diodes (LEDs) owing to their ease of solution processing and high color purity. Furthermore, current QD light-emitting diodes (QLEDs) exhibit high electroluminescence performance and lifetime comparable to those of organic LEDs. However, some challenges remain in the commercialization of QLEDs for next-generation displays. One key issue is that blue QLEDs exhibit lower efficiency and lifetimes compared to red and green QLEDs, which is attributed to a deep valence band and wide bandgap. In this study, we discuss recent developments that aim to enhance the efficiency of blue QLEDs and explore the challenges that must be addressed for their commercialization.

Keywords Quantum dot light-emitting diodes · Blue quantum dots · Electroluminescence · Device structures · Degradation mechanism

Introduction

Quantum dots (QDs) have garnered significant attention and have been applied in various optoelectronic fields, such as light-emitting diodes (LEDs), photovoltaics, and lasers, owing to their narrow full width at half maximum (FWHM), high photoluminescence quantum yield (PLQY), and ease of synthesis into precise and uniform sizes through hot injection [1–8]. Particularly, QDs can easily control the emitted color by adjusting the core size, making them an ideal choice for LEDs that require a combination of red, green, and blue to achieve full color [9–13].

Early work on QLEDs, reported by Coe et al. in 2002, showed an external quantum efficiency (EQE) of only around 1%. However, substantial progress has been made in improving the efficiency of QLEDs through various approaches, including QD engineering methods, such as the introduction of intermediate shells into QDs [14], the

use of giant shells [15, 16], and methods to improve charge injection, such as aligning the energy level of the charge-transfer layer to facilitate smooth charge injection into QDs [17, 18], and interlayer insertion methods [17, 19]. In 2013, Yang et al. reported on red QLEDs with an EQE exceeding 20%, and demonstrated the potential for QLEDs to outperform organic LEDs (OLEDs) in terms of efficiency [20, 21]. In addition, unlike OLEDs, which are typically fabricated using a thermal evaporator, QLEDs offer a cost advantage by being fabricated through an all-solution process. Therefore, QLEDs are considered as next-generation display poised to replace OLEDs, which suffer from cost disadvantages [22–27]. To date, the highest reported EQEs of red and green QLEDs were 33.1% [28] and 28.7% [29], respectively, and the half lifetime at 100 cd m⁻² (T_{50}) were over 100,000,000 and 1,000,000 h, respectively, exhibiting excellent efficiency and lifetime sufficient for commercialization [30, 31].

Despite these advancements, there are still some points that require improvements to facilitate the commercialization of QLEDs. Specifically, improving the performance of blue QLEDs is crucial, as they currently exhibit lower efficiency and shorter lifetimes than red and green QLEDs. In 2018, Wang et al. reported a deep blue QLED with an EQE of 18.0% and a peak electroluminescence (EL) spectrum of 445 nm obtained by introducing a Cd_xZn_{1-x}S intermediate shell into a ZnCdS core [32]. In addition, Wang et al.

Youngwoo Jeon and Hyungsuk Ryu have contributed equally to this work.

✉ Hyunho Lee
hyunho@kw.ac.kr

¹ Department of Electronic Engineering, Kwangwoon University, Seoul 01897, Republic of Korea

reported a CdSe/ZnS blue QLED with an EQE of 19.8% by introducing a thick ZnS shell and substituting zinc oxide (ZnO), which was previously used as an electron-transport layer (ETL) with a smaller size [33]. Despite significant advancements in achieving a maximum EQE close to 20%, the T_{50} of the aforementioned devices (both at 47.4 h) were considerably shorter than those of the red and green QLEDs. In 2023, Chen et al. reported a ZnCdSe/ZnSeS/ZnCdS/ZnS blue QLED with an EQE of 20.4% and a T_{50} of 80,377 h, which was the highest efficiency among Cd-based blue QLEDs reported thus far [34]. However, its lifetime still being considerably shorter than that of previous red and green QLEDs (100,000,000 and 1,000,000 h, respectively) with a difference of two orders of magnitude, even though it employs toxic-material, Cd-based QDs. Therefore, further improvement of blue QLEDs is an essential part of making QLEDs commercially viable as a replacement for OLEDs. In particular, the lifetime of QLEDs must be significantly enhanced to meet more than the minimum lifetime of 30,000 h required for commercialization [35].

The reasons for the lower efficiency and shorter lifetime of blue QLEDs compared to those of red and green QLEDs are as follows: (i) A wide bandgap is essential to emit light with short wavelengths (<495 nm). (ii) Deep valence band (VB) maximum makes it difficult to inject holes. (iii) The difficulty in synthesizing uniform sizes of QDs arises from the small-core size of blue QDs (as in the case of CdSe blue QD, <2 nm) [36–38]. To address these issues, substantial

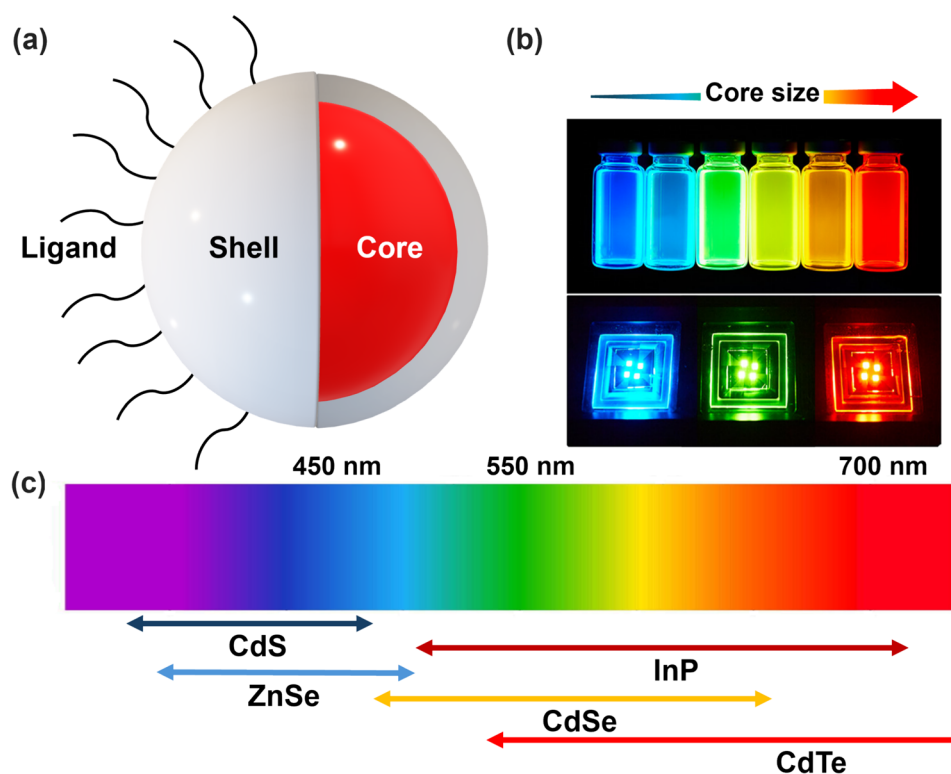
improvements are required in various aspects, such as material, structure, and interface engineering of QDs and LED devices. This review summarizes the advancements in materials and device engineering for blue QLEDs and analyze the degradation mechanisms that enhance the lifetime of blue QLEDs.

Progress in Materials of Blue-Emitting QDs

Material Physics of QDs

As shown in Fig. 1a, QDs are composed of three parts: (i) Core that emits light with a wavelength corresponding to the bandgap, (ii) shell that wraps around and protects the core, (iii) ligand that facilitates the dispersion of QDs in organic solvents and protects QDs. The core plays a central role in emitting light in the LED, but when it is solely composed of the core, it responds very sensitively to factors, such as surface defects and humidity, resulting in a short lifetime of only a few seconds [39, 40]. To address this issue, a shell was introduced, which surrounded the core to prevent the core from being degraded by external conditions and to ensure stable operation, as well as to passivate defects and dangling bonds on the core surface [30, 37]. Ligands provide the necessary colloidal stability and solution processibility for QDs, while also passivating surface defects [25, 37]. These QDs exhibit size-dependent color emission

Fig. 1 Characteristics of quantum dot (QD). **a** Schematic showing the shape of QD. **b** QD solutions with different core sizes. Reproduced with permission [13]. Copyright 2023, American Chemical Society. **c** Representative QD's core materials and their emission spectrum



owing to the quantum confinement effect. When the core size becomes smaller than the inherent exciton Bohr radius, the bandgap of the material becomes inversely proportional to its size [41]. In other words, QDs made of the same material can emit different colors of light depending on the core size. Schematic of QD, different core size QDs, and their applications in QLEDs are shown in Fig. 1b [13]. There is a limit to the spectral range that a material can have owing to its intrinsic exciton Bohr radius. A schematic of the spectral range of a material is shown in Fig. 1c [42].

Components of the Blue QD Core

Figure 2a shows the emission wavelengths and energy band diagrams of the red, green, and blue QDs. As mentioned above, QDs emit light of wavelengths inversely proportional to their size owing to the quantum confinement effect. Blue QDs, which require shorter wavelengths than red and green QDs, have smaller core sizes, wider optical bandgaps, and deeper VBs. These factors not only make it difficult for holes to be injected into the emission layer in blue QLEDs, but also have adverse effects on efficiency, such as quenching and PLQY [51, 52]. In addition, during the synthesis of QDs, the growth kinetics of nucleation, reaction time, and use of multiple ligands, as well as the additional injection of precursors, need to be adjusted with complexity and precision [37]. However, as shown in Fig. 2b and c, the core size of blue QDs is much smaller than those of red and green QDs, making it difficult to obtain them under conventional reaction conditions and challenging to synthesize uniform QDs, leading to instability. For these reasons, blue QLEDs show much lower performance compared to red and green

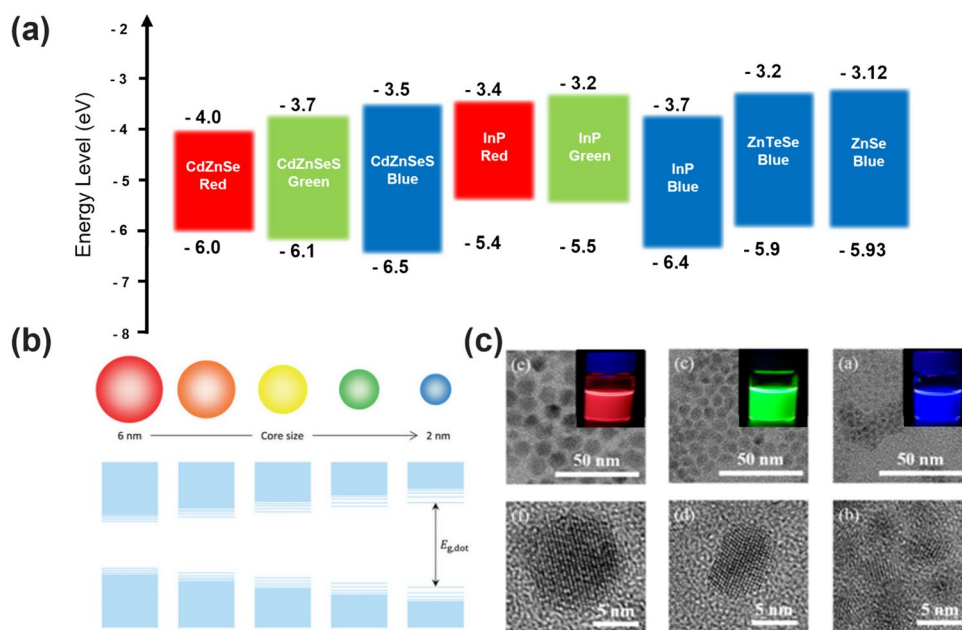
QLEDs, and extensive research is ongoing to improve their performance. Therefore, careful selection and modification of materials that constitute QDs is essential.

Cd-Based Blue-Emitting QD

Cd-based QDs have several favorable characteristics, including a proper direct bandgap of 1.73 eV, abundant precursor choices, and controllable size with uniform nanoscale dimensions [26, 53]. In addition, Cd-based red and green QDs exhibit excellent PL properties, such as a PLQY close to 100%, narrow FWHM, and remarkable stabilities [25, 54]. Based on these advantages, Cd-based red and green QLEDs reported very high efficiencies of 20.5% and 12.6%, respectively, in 2014 [14, 19]. Therefore, several researchers have selected Cd-based QDs as materials for blue QLEDs.

In the early stages, Cd-based blue QLEDs exhibited a very low efficiency, with a PLQY of approximately 50% and an EQE of approximately 0.3% [57, 58]. In 2014, Shen et al. synthesized high-quality violet-blue QDs with a high PLQY of approximately 100% by adjusting the Zn content of $Zn_xCd_{1-x}S/ZnS$ core/shell QDs and utilizing a high-temperature shell growth method (Fig. 3a, b) [55]. This method promotes the rapid growth of shells and facilitates the diffusion of S and Zn atoms into the $Zn_xCd_{1-x}S$ core regions, resulting in the restoration of the surface of the $Zn_xCd_{1-x}S$ cores and the formation of consecutive changes in lattice parameters with $Zn_xCd_{1-x}S$ buffer layers, thus avoiding stress defects. The QLEDs using $Zn_xCd_{1-x}S/ZnS$ core/shell QDs also exhibited a high EQE of 3.8%. In 2015, Shen et al. replaced the oleic acid surface ligand of QDs with 1-octanethiol, consequently reducing the center-to-center distance

Fig. 2 **a** Energy level diagram of red, green, and blue CdZnSe QD; [43] red, green, and blue InP QD; [44–46] and blue ZnSe and ZnTeSe QD [47, 48], **b** bandgap of QDs as a function of diameter. Reproduced with permission [49]. Copyright 2023, Wiley–VCH. **c** TEM image of CdSe/ZnS core/shell QDs with various peak emission wavelengths (left: 630 nm, red; middle: 520 nm, green; right: 450 nm, blue). Reproduced with permission [50]. Copyright 2015, Optica Publishing Group



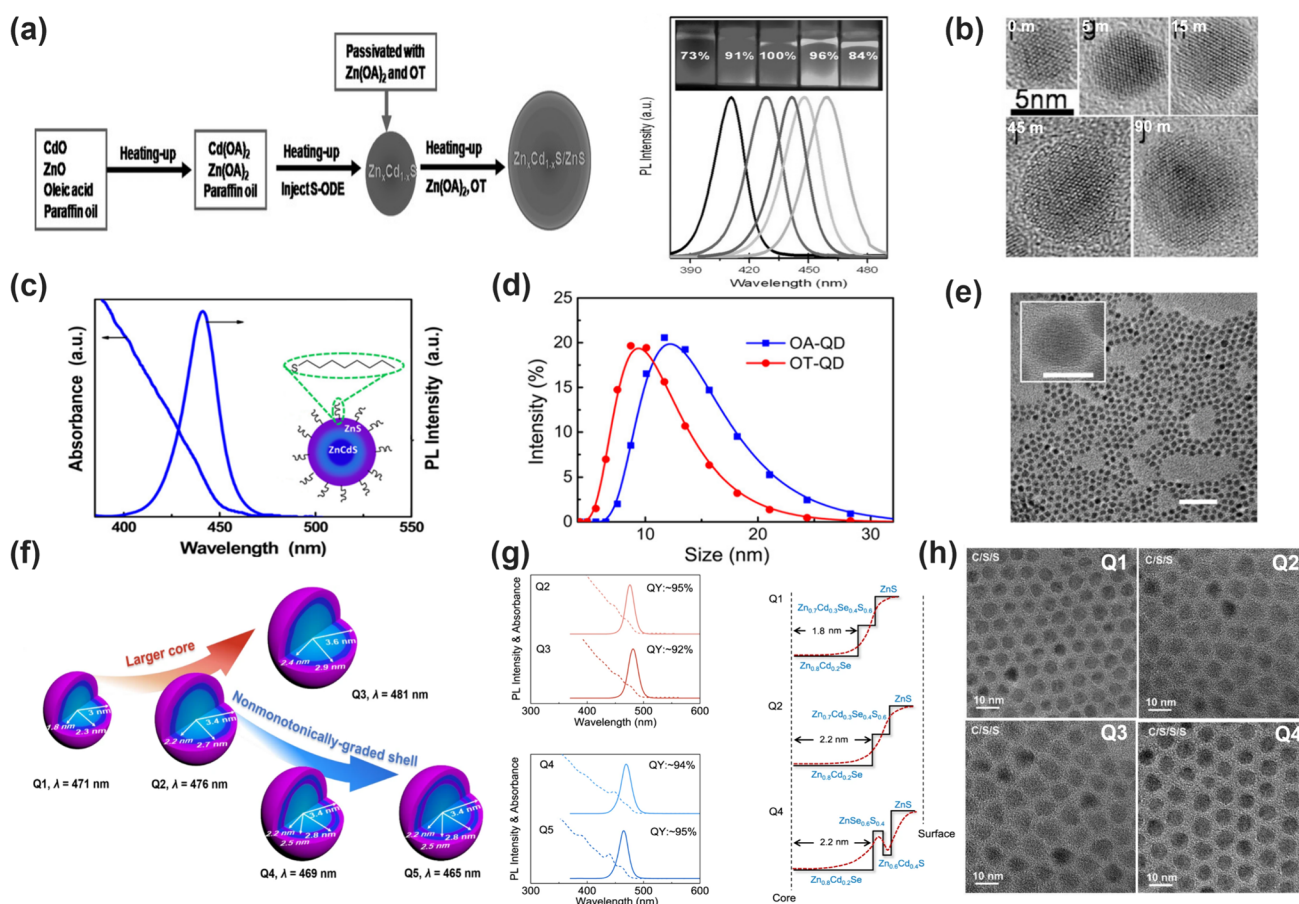


Fig. 3 **a** The synthetic procedure of $\text{Zn}_x\text{Cd}_{1-x}\text{S}/\text{ZnS}$ core/shell QDs and its PLQY and normalized PL spectra with different x . **b** TEM image of $\text{Zn}_{0.25}\text{Cd}_{0.75}\text{S}$ core/shell QDs with various shell growth times (0–90 min). Reproduced with permission. [55] Copyright 2014, Wiley–VCH. **c** Absorption and PL spectra of ZnCdS/ZnS QDs and **d** dynamic light scattering spectra of ZnCdS/ZnS QDs with oleic

acid and 1-octanethiol ligands. **e** TEM image of ZnCdS/ZnS QDs. Reproduced with permission. [56] Copyright 2015, American Chemistry Society. **f** Core/shell structures and **g** schematic diagram of the conduction band minimum of QDs. **h** TEM image of Q1–Q4 QDs. Reproduced with permission. [34] Copyright 2020, Nature Publishing Group

between the QDs and increasing the electron mobility by nearly twofold (Fig. 3c,d,e) [56]. This enhancement resulted in improving the charge injection properties of the deep blue ZnCdS QDs, resulting in QLEDs with a maximum EQE of 12.2%.

However, the lifetime of Cd-based blue QLEDs remains limited to only several hours to tens of hours, indicating the need for improvement. In 2015, Yang et al. improved the charge injection and suppressed non-radiative Auger recombination by thinning the ZnS outer shell of $\text{Zn}_x\text{Cd}_{1-x}\text{S}$ QDs, thereby enhancing the lifetime of QLEDs [21]. QLEDs exhibited a high EQE of 10.7% and enhanced T_{50} of 1000 h. In 2020, Pu replaced the carboxylate and cadmium carboxylate ligands of $\text{CdSeS}/\text{ZnSeS}/\text{ZnS}$ QDs with electrochemically inert fatty amine ligands (RNH_2), bridging the PL–EL gap. This resulted in an enhancement in the performance of blue QLEDs, achieving an EQE of 8.05%, a high luminance of $62,600 \text{ cd m}^{-2}$, and a T_{50} of 10,000 h [59].

Despite these improvements, Cd-based blue QDs still exhibited a significantly shorter lifetime than red and green QLEDs owing to challenges, such as difficulties in synthesizing uniform QDs caused by their small particle size, and the sensitivity of exciton traps resulting from the wide bandgap, leading to non-radiative recombination [60]. In 2023, Chen et al. enlarged the core size and introduced an intermediate shell to ensure that the QDs had non-monotonically graded energy levels, reducing surface-bulk coupling and tuning the emission wavelength without compromising charge injection (Fig. 3f) [34]. The large-core $\text{ZnCdSe}/\text{ZnSeS}/\text{ZnCdS}/\text{ZnS}$ blue QDs exhibited a high PLQY (approximately 95%) and deep blue peak emission at 465 nm (Fig. 3g, h). The corresponding QLED achieved a maximum EQE of 20.4% and a T_{50} of 80 377 h, demonstrating that Cd-based blue QLEDs possess sufficient lifetime and efficiency to enter the commercialization stage.

Cd-Free Blue-Emitting QDs

As mentioned above, Cd-based blue QLEDs have achieved high efficiency with EQE exceeding 20% and reported lifetimes exceeding 80,000 h. This result signifies that the performance of the blue QDs reaches the level of OLEDs. However, owing to the restriction of hazardous substances regulation, the inherent toxicity of heavy-metal QDs, including Cd, limits their commercialization. Therefore, several materials are being studied to replace them. Among potential candidates, InP-QDs, which have been used to replace Cd-based QDs in red and green QLEDs, have been researched [61].

In 2017, Shen et al. synthesized InP/ZnS small-core/thick-shell tetrahedral-shaped QDs that exhibited a high PLQY of 76.1% and a long PL lifetime of over 1000 h. However, blue InP QLEDs utilizing these QDs achieved a maximum luminance of 90 cd m^{-2} [65]. In 2020, Zhang et al. addressed the lattice mismatch between the core and shell of InP/GaP/ZnS QDs by introducing GaP as the inner shell (Fig. 4a, b). In addition, they optimized the thickness of the ZnS outer shell to balance charge injection. Based on this, QD shows a PLQY of 81% and the QLEDs exhibited an EQE of 1.01% and a maximum luminance of 3120 cd m^{-2} , which is the highest reported luminance among blue InP QLEDs, thus far [62]. In 2020, Zhang utilized zinc oleate and S-TOP precursors to epitaxially grow a second ZnS shell (Fig. 4c), reducing surface defects and improving the PLQY (18% to 45%) and PL lifetime (36.2 ns to 45.1 ns) of the QDs (Fig. 4d). The QLEDs exhibited a maximum EQE of approximately 1.7%, marking a threefold improvement compared to the previous value of 0.6% [61]. In addition, in 2020, Kim et al. used the aminophosphine precursor P(DMA)₃ to synthesize InP-QDs by adjusting the reaction times and sequentially surface-passivating them with ZnSeS inner and ZnS outer shells, resulting in InGaP QDs exhibiting a deep blue PL at 465 nm and a PLQY of 80% (Fig. 4e, f). In addition, QLEDs using InGaP QDs exhibited an EQE of 2.5% and a maximum luminance of 1038 cd m^{-2} [63].

Despite these efforts, the performance of blue InP QLEDs remains poor, with a maximum EQE of approximately 2.8%. This could be attributed to various challenges, such as the difficulty in controlling the synthesis of small InP cores (< 3 nm) and the epitaxial growth of shells. Moreover, the emitted colors range from azure to sky blue, indicating a poor color quality [66, 67]. In contrast to InP-QDs, ZnSe-based QDs are gaining attention as emerging blue QD materials, offering eco-friendliness, larger core sizes than Cd-based and InP QDs, and inherent proficiency in emitting blue light with a narrow FWHM [68].

In 2012, research on ZnSe-blue QLEDs exhibited low efficiencies, with EQEs of approximately 1% and a maximum luminance of 1000 cd m^{-2} , owing to issues such as

the large bandgap (approximately 2.7 eV) and deep VB of ZnSe [69, 70]. In 2015, Wang et al. synthesized ZnSe/ZnS core/shell QDs by introducing low-temperature nucleation and high-temperature shell growth methods, which effectively passivated surface defects. In addition, they utilized octanethiol stock solution as the S-precursor instead of S-ODE (1-octadecene), resulting in the synthesis of high-quality and stable QDs with a PLQY of over 80% [71]. QLEDs utilizing these QDs exhibited a maximum luminance of 2632 cd m^{-2} and EQE of 7.83%. In 2021, Gao et al. synthesized ZnSe/ZnS core/shell QDs with bulk-like size ZnSe cores and thin ZnS shells, resulting in a minor bandgap distribution, near-unity PLQY (approximately 95%), and long PL lifetime characteristics (Fig. 4g, h). QLEDs utilizing these QDs also exhibited a high EQE of 12.2% and T_{50} of approximately 237 h [64].

However, ZnSe QDs face challenges owing to their wide bandgap, leading to emission peaks primarily concentrated in the blue–violet region and difficulty in effectively passivating the surface on excessively large cores [66, 72]. To address this issue, a new method was introduced to effectively adjust the bandgap by synthesizing ternary ZnTeSe QDs by alloying ZnSe with ZnTe, which has a relatively narrow bandgap (2.25 eV) [66].

In the early stages, ZnTeSe QDs faced challenges, including lattice defects owing to the different ion radius of Te and Se, as well as a broad emission spectrum stemming from non-uniform Te distribution, resulting in a low PLQY (< 30%) and broad FWHM (> 75 nm). [30, 72, 73]. In 2019, Jang et al. synthesized ZnSeTe/ZnSe/ZnS QDs with a PLQY of 70% and a narrow FWHM of 32 nm by optimizing the Te/Se ratio and ZnSe inner shell thickness. (Fig. 5a, b, c) [73]. In 2020, Kim et al. introduced HF and ZnCl₂ additives, where HF facilitates the separation of ligands through protonation and effectively etched away the surface oxidation states, whereas ZnCl₂ is found to control the growth direction of the initial ZnSe shell (Fig. 5d) [74]. Using these methods, the improved ZnTeSe QDs achieved a high-quality PLQY of approximately 100% (Fig. 5e), whereas the ZnTeSe-QLEDs demonstrated an impressive EQE exceeding 20%, an EL peak wavelength of 460 nm, a maximum luminance of $88,900 \text{ cd m}^{-2}$, and a record-breaking T_{50} at 100 cd m^{-2} , reaching 15,850 h. In 2022, Lee et al. synthesized high-quality QDs with a maximum PLQY of 96% and demonstrated a high EQE of 18.6% in the resulting QLED by modulating the thicknesses of the ZnSe inner and ZnS outer shells and the Te/Se composition ratio in the ZnSeTe core (Fig. 5f, g, h) [75]. As such, ZnTeSe QLEDs exhibited long lifetimes of over 10,000 h and high efficiencies of over 20%, demonstrating that ZnTeSe QDs are potential candidates to replace Cd-based blue QDs in the next generation.

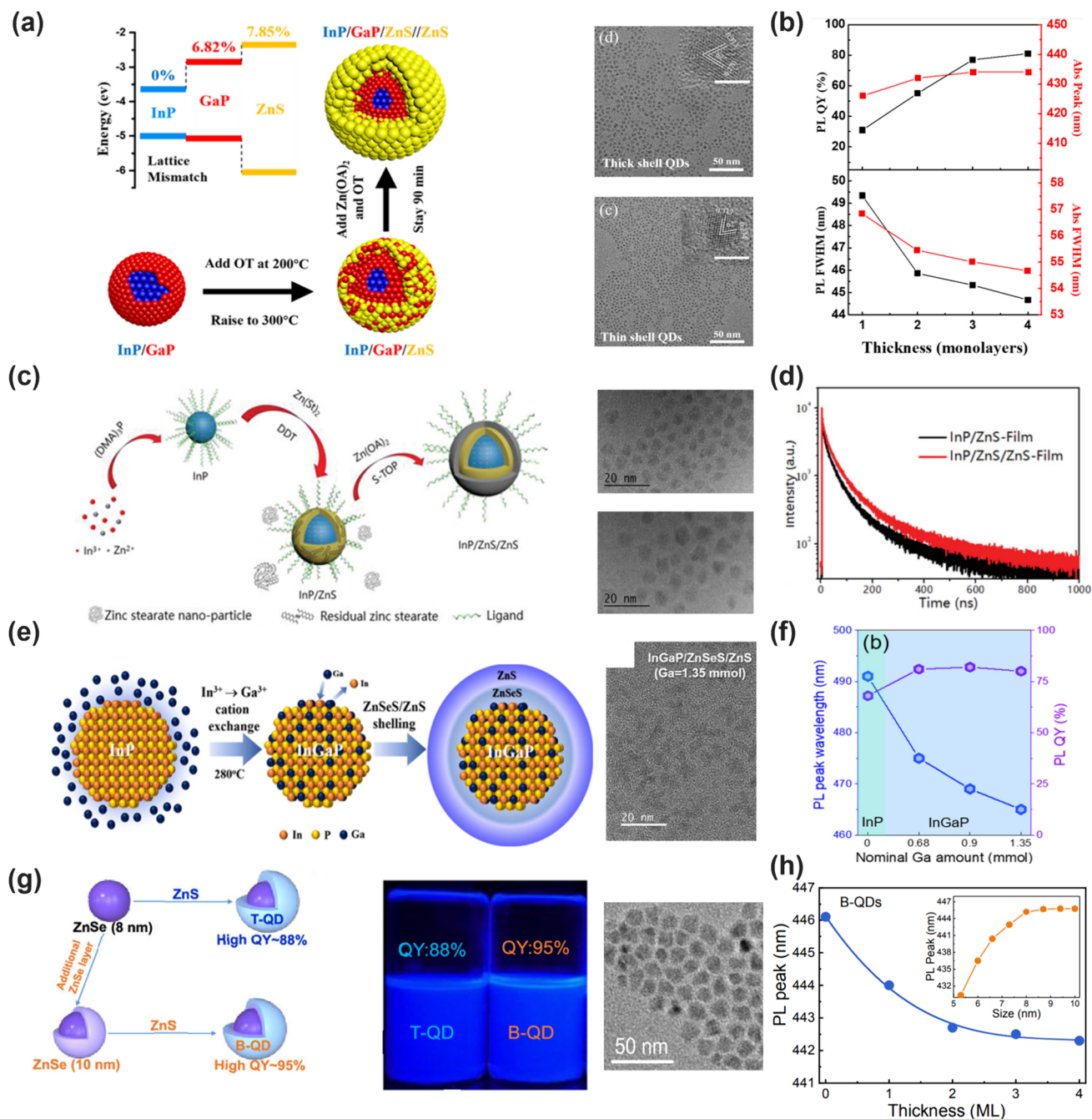


Fig. 4 **a** Synthesis process and energy band diagram of thick-shell InP/GaP/ZnS blue QDs and their corresponding HRTEM images. **b** PL and absorption characteristics of InP/GaP/ZnS blue QD as a function of ZnS shell thickness. Reproduced with permission. [62] Copyright 2020, American Chemistry Society. **c** Schematic of the synthesis process for thick-shell InP/ZnS/ZnS QDs and their corresponding HRTEM images. (Top: InP/ZnS, Bottom: InP/ZnS/ZnS). **d** Time-resolved PL decay traces of InP/ZnS and InP/ZnS/ZnS films. Reproduced with permission. [61] Copyright 2020, Wiley-VCH. **e** Schematic illustration of cation exchange-based InGaP/ZnSeS/ZnS QD

and TEM image of Ga=1.35 mmol-based InGaP/ZnSeS/ZnS QDs. **f** PL peak wavelength and PLQY of InGaP/ZnSeS/ZnS QDs depending on Ga₃ amount. Reproduced with permission. [63] Copyright 2020, American Chemistry Society. **g** Schematic of the controlled synthesis of two types of QDs, traditional ZnSe/ZnS QDs (T-QD) and bulk-like ZnSe/ZnS QDs (B-QD) and TEM image of B-QD. **h** Emission peak wavelength of B-QDs as a function of ZnS shell thickness. Inset: Emission peak wavelength of ZnSe QDs as a function of core size [64]. Reproduced with permission. Copyright 2021, American Chemistry Society

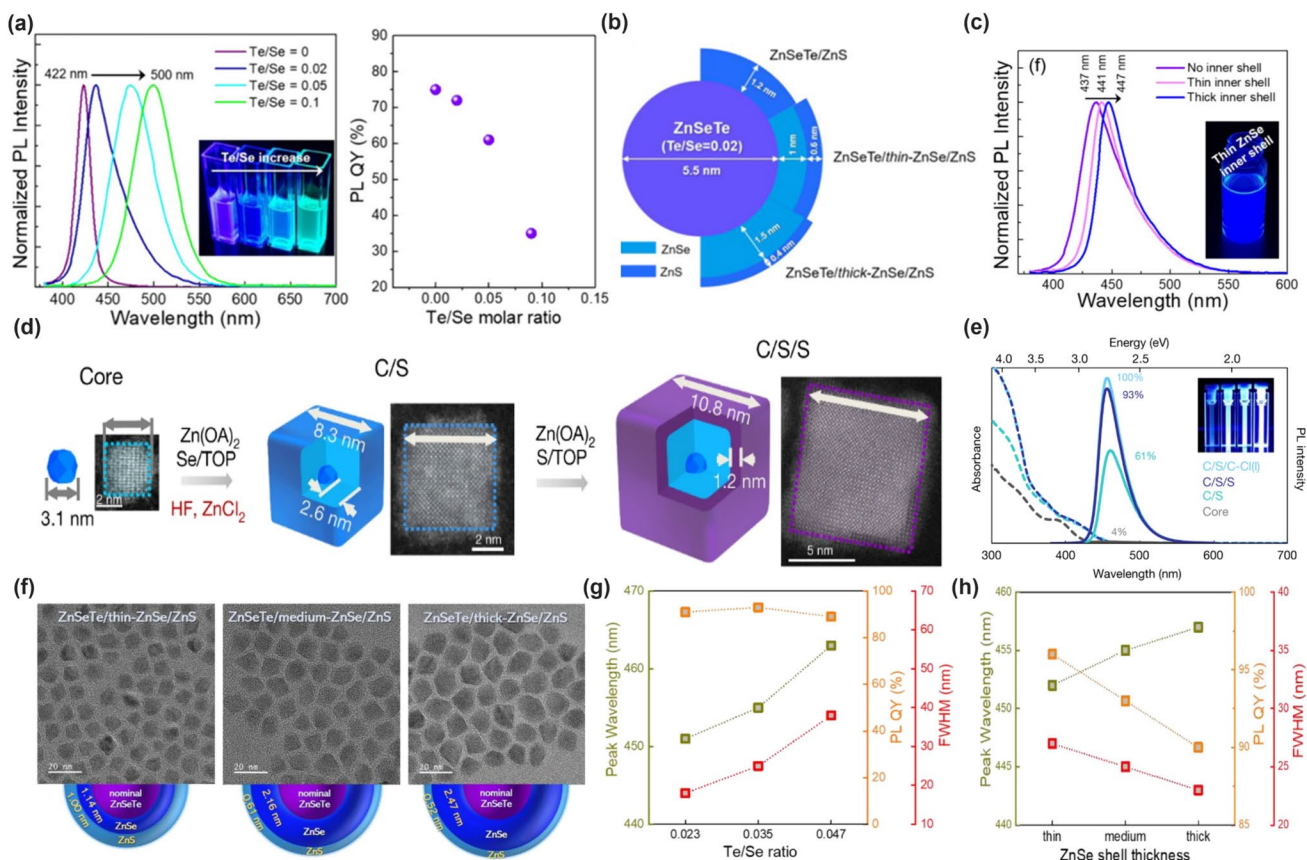


Fig. 5 **a** Normalized PL spectra and PLQY of ZnTeSe/ZnSe/ZnS QDs based on Te/Se molar ratio. **b** Dimensional information of double-shelled ZnSeTe/thin- or thick-ZnSe/ZnS QDs. **c** PL spectra of ZnSeTe/ZnSe/ZnS QD with different inner shell thicknesses. Reproduced with permission [73]. Copyright 2019, American Chemical Society. **d** Schematic of synthesis of ZnTeSe, ZnTeSe/ZnSe, and ZnTeSe/ZnSe/ZnS QDs. **e** Absorption and PL spectra of QDs. Inset:

Photograph taken under illumination at 365 nm. Reproduced with permission [74]. Copyright 2020, Nature Publishing Group. **f** TEM images and dimensional information of ZnSeTe/thin-, and thick-ZnSe/ZnS QDs, **g** PL characteristics of ZnSeTe/medium-ZnSe/ZnS QD with different Te/Se molar ratios, and **h**) ZnSe shell thickness. Reproduced with permission [75]. Copyright 2022, Elsevier

Device Engineering

Figure 6a shows that the blue QDs have significantly broader bandgap than the green and red QDs. In addition, high-performance blue QLEDs often utilize blue QDs with thicker shells, which further extends the bandgap and complicates the charge injection process. Consequently, the deeper VB level inherent in blue QDs leads to a substantial barrier to hole injection at the HTL/QD interface while simultaneously presenting a negligible barrier to electron injection. This disparity culminates in a marked imbalance in charge injection, contributing to an increased QD charging and turn-on voltage for blue QLEDs [76]. To improve this, the HTL requires a deeper highest occupied molecular orbital (HOMO) level than that typically utilized in red and green QLEDs, paired with a strategy to mitigate the overabundance of electron injection in the ETL. To address this challenge of charge injection imbalance, materials that exhibit properties that foster a more equitable charge injection

dynamics are required. Moreover, in the ETL, the materials must be selected to restrain excess electron injection. Potential candidates for overcoming this issue are shown in Fig. 6b. To fabricate efficient blue QLEDs, it is imperative to fine tune these candidates to harmonize them with the specific requirements of blue QDs.

Facilitating Hole Injection

The primary cause of the charge imbalance in blue QLEDs is the deep VB of the blue QDs. Consequently, numerous studies have been conducted on the development of HTLs with deeper HOMO levels. In 2012, Xiang et al. replaced the poly(4-butylphenyl-diphenyl-amine) (poly-TPD) with poly(9-vinylcarbazole) (PVK) to reduce the hole injection barrier of blue QD's VB (6.6 eV) from 1.4 to 0.8 eV [70]. This modification resulted in improved turn-on voltage (from 4.4 to 3.5 V) and EQE (from 0.3 to 0.65%). In 2010, Ho et al. compared the potential of various organic

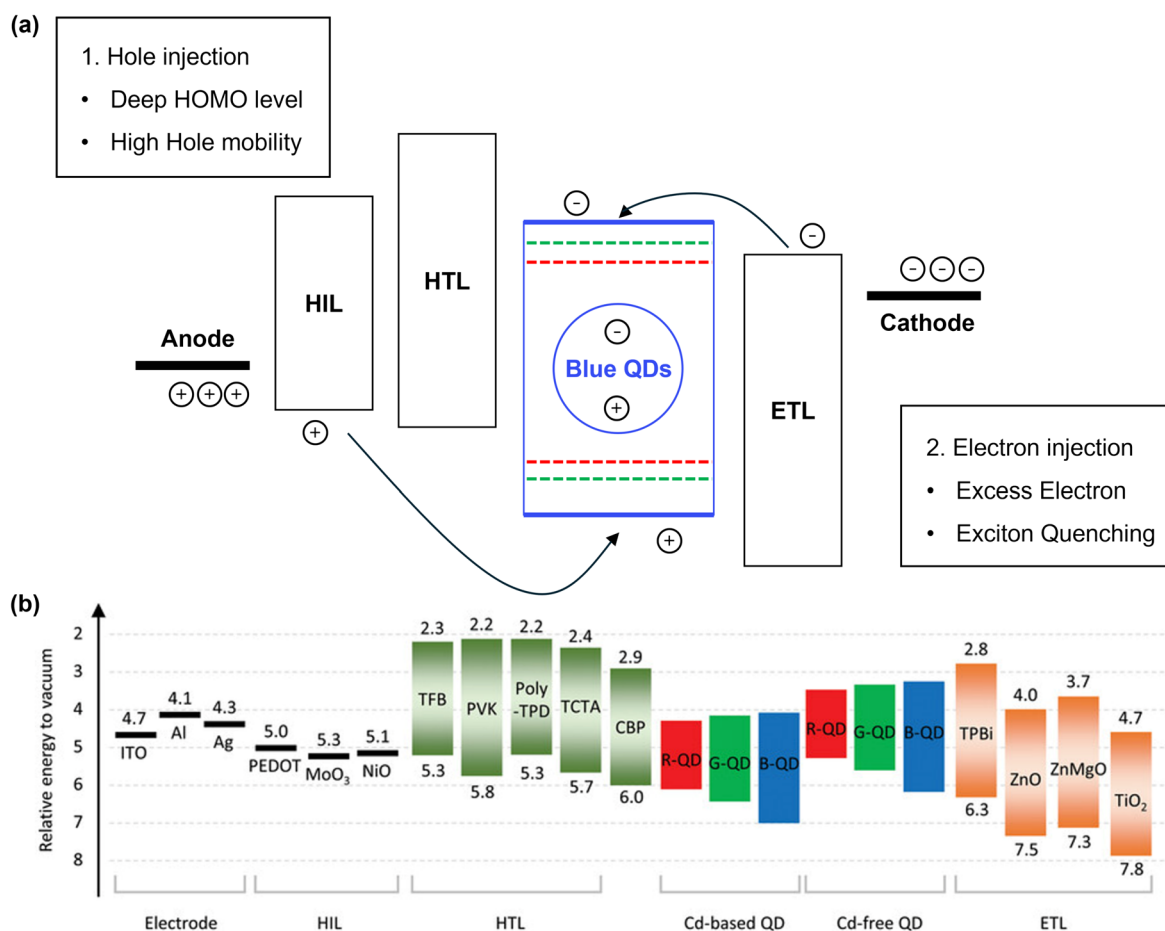


Fig. 6 **a** Strategic design and operation mechanism of a QLED with blue QDs. The diagram illustrates the strategy of aligning the energy levels of the ETL and hole transport layer (HTL) with those of blue QDs' energy levels to ensure efficient charge injection and transport.

b Energy band diagram depicting typical configuration of QLEDs. This diagram includes commercial materials commonly used in the construction of QLEDs, highlighting the relative energy levels of QDs. Reproduced with permission [49]. Copyright 2023, Wiley-VCH

Table 1 Comparison of HTMs for blue QLED applications

HTMs	HOMO [eV]	LUMO [eV]	Hole mobilities [$\text{cm}^2 \text{V}^{-1} \text{s}^{-1}$]	References
PVK	5.8	2.2	2.5×10^6	[78]
Poly-TPD	5.2	2.3	1.0×10^4	[79]
TPD	5.5	2.3	1.1×10^3	[78, 80]
TCTA	5.7	2.4	2.0×10^5	[78, 80]
CBP	6.0	2.9	1.0×10^3	[80, 81]
TFB	5.4	2.3	2.0×10^{-3}	[82]

polymers and small molecules as hole transporting materials (HTMs), summarized in Table 1, which reveal that among polymers, PVK exhibits the deepest HOMO level, leading to the highest luminance and current efficiency [77]. However, its low hole mobility contributed to a problematic high turn-on voltage (6.5 V). Despite their high hole mobility

and deep HOMO levels, small molecules like (*N,N'*-bis(3-methylphenyl)-*N,N'*-diphenylbenzidine (TPD), tris(4-carbazoyl-9-ylphenyl)amin (TCTA), or 4,4'-Bis(*N*-carbazoyl)-1,1'-biphenyl (CBP)) are unsuitable for QLED applications owing to their low packing density when in thin film. To decrease PVK's turn-on voltage, high-mobility small molecules (TCTA, CBP, or TPD) were added to improve hole mobility. Notably, TCTA, with a relatively high glass transition temperature (T_g) of approximately 151 °C, did not crystallize like the other materials and effectively enhanced the EL performance of the QLEDs, achieving a lower turn-on voltage (5 V), higher current efficiency (14 cd A^{-1}), and increased luminance ($44,000 \text{ cd m}^{-2}$). These results indicate that HTLs must possess high hole mobility and deep HOMO levels.

As shown in Table 1, finding a material that simultaneously possesses a high hole mobility and a deep HOMO level is challenging. To address this issue, in 2015, Lin et al. utilized a PVK/Poly[(9,9-dioctylfluorenyl-2,7-diyl)-*co*-(4,4'-

(N-(4-s-butylphenyl)diphenylamine)] (TFB) mixture with high hole mobility and recorded an EQE of 7.39% and a maximum luminance of 2856 cd m^{-2} [84]. They demonstrated that a specific ratio of TFB and PVK could enhance turn-on voltage, luminance, and efficiency. In 2016, Wang et al. constructed a blue QLED using TFB as the HTL and mixed QDs with PVK, reaching an EQE of 8.76% and a maximum luminance of 13,800 cd m^{-2} [85]. The mixed QD layer acted as a donor to the TFB and PVK, improving exciton energy transfer from the organic host to the QDs. In 2022, Cheng et al. doped TFB with PVK, leading to increased hole mobility and a slight downward shift in the HOMO level, which was attributed to the increased π - π stacking intensity, leading to enhanced hole injection [86]. However, using HTL bilayer is challenging owing to the difficulty of depositing HTL without compromising the integrity of the underlying layer. Chen et al. used chlorobenzene

(CB) as a solvent and optimized the single and bilayer (PVK/TFB) HTLs to a suitable thickness, achieving a high EQE of 5.9% and a low turn-on voltage of 2.6 V [87]. Liu Yu et al. used a bilayer HTL of solution-processed PVK(1,4-dioxane)/TFB(p-Xy) in an inverted structure, reducing the turn-on voltage to 4.1 V and achieving a luminous efficiency of 5.99% [88]. Both studies demonstrated that a bilayer HTL can improve the hole injection, block electron overflow, and suppress exciton quenching, leading to enhanced device performance. Although the bilayer is a good strategy for improving hole injection, proper solvent selection for PVK is still a major challenge for the TFB/PVK bilayer to ensure that the integrity of the underlying TFB layer is not compromised during PVK deposition. In 2021, Chen et al. compared the PVK layers stacked on TFB using various solvents (Fig. 7a) [82]. DMF was found to be the most suitable orthogonal solvent for TFB(CB), according to the PL spectra

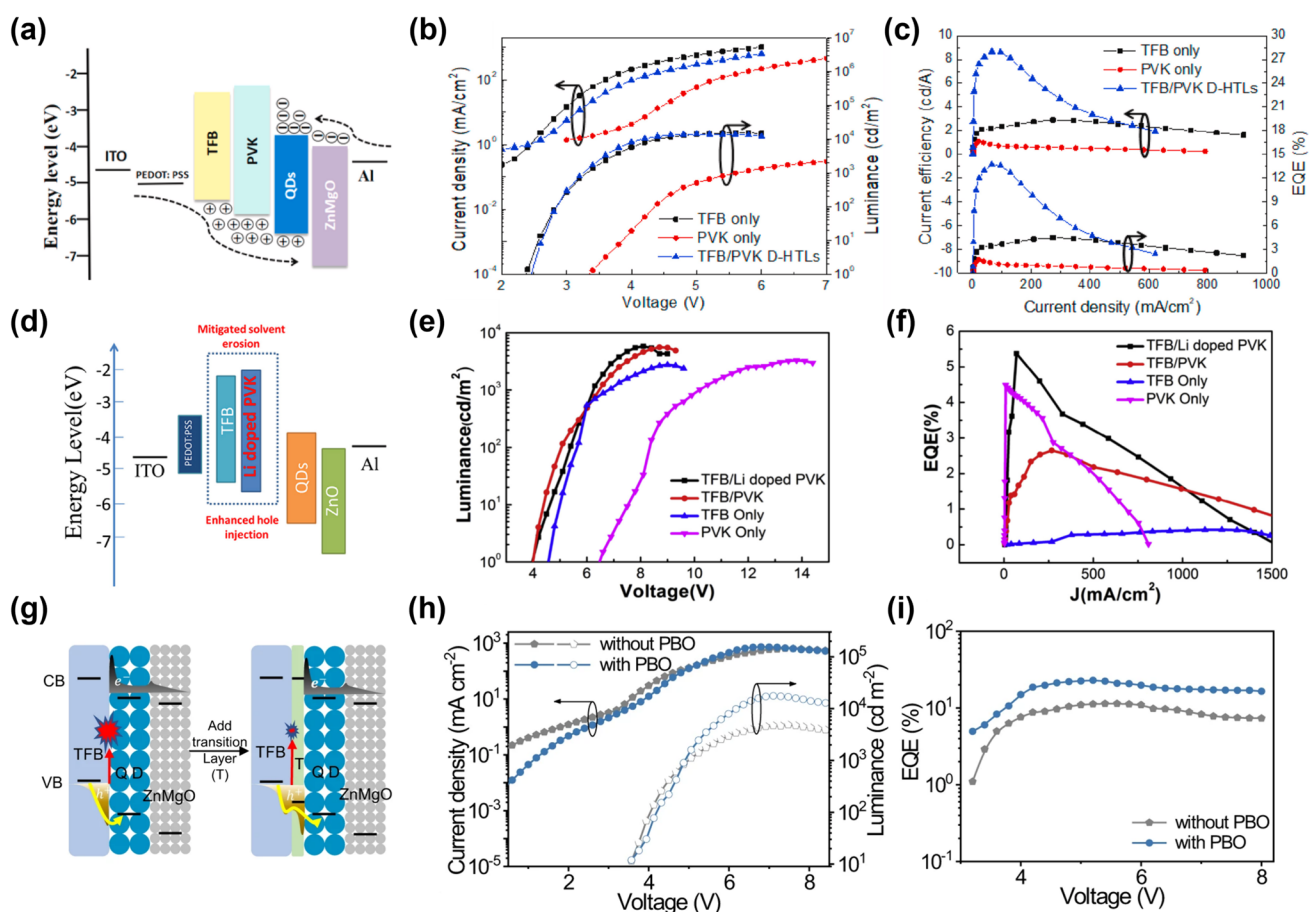


Fig. 7 a Energy band diagram for QLEDs incorporating dual-function HTLs (D-HTLs). b Current efficiency and EQE of QLEDs with various HTL. c Current efficiency and EQE of QLEDs with various HTL. Reproduced with permission [82]. Copyright 2021, Elsevier. d Energy band diagram of QLEDs with TFB and Li-doped PVK as HTL. e L-V characteristic and f EQE of QLEDs using single and bilayer HTLs. Reproduced with permission [83]. Copyright 2020,

Elsevier g Schematic illustration of damage to the hole-transport layer (HTL) caused by the carrier accumulation without and with a transition layer. h The current density–luminance–voltage characteristics and i external quantum efficiency (EQE) as a function of voltage for the QLEDs without and with PBO. Reproduced with permission. [44] Copyright 2024, Nature Publishing Group

and AFM analysis. The optimized blue QLED using TFB/PVK(DMF) exhibited a low turn-on voltage similar to that of TFB alone and demonstrated maximum CE and EQE of 8.64 cd A^{-1} and 13.7%, respectively, as shown in Fig. 7b, c. This finding is attributable to the improved charge balance, as is evident from the HOD comparison. In 2020, Zheng et al. aimed to improve hole injection more by doping HTLs and introducing a TFB/Li-PVK bilayer as the HTL (Fig. 7d) [83]. Consequently, they recorded a maximum luminance of 5829 cd m^{-2} and maximum EQE of 5.37% (Fig. 7e, f).

Unbalanced carrier injection is critical in degrading the performance of blue QLEDs. However, traditional methods for improving hole injection, such as using HTLs with a lower HOMO level, have limitations owing to the energy level alignment and potential device degradation. Therefore, effective strategies that involve the introduction of additional layers, such as MoO_3 or an anti-oxidation layer, to enhance hole injection and transport, leading to balancing carrier injection, are also being pursued for efficient blue QLEDs. In 2021, Tan et al. introduced an ultrathin MoO_3 electro-dipole layer between the hole injection layer and HTL, creating a built-in electric field with forward dipoles that strengthens hole injection and facilitates carrier balance. [44] However, the p-doping effect of MoO_3 leads to increased carrier concentration and reduced trap density at the interface HTL, enhancing the effective hole mobility. Consequently, the maximum external quantum efficiency of the blue InP QLED increased from 1.0 to 2.1%. In 2024, Zhang, Wenjing, et al. suggested the incorporation of an anti-oxidation layer poly(p-phenylene benzobisoxazole) (PBO) between interfaces to harvest some holes from the HTL (Fig. 7g), mitigating oxidation-induced device degradation and enabling a T_{50} of over 41,000 h at an initial luminance of 100 cd m^{-2} for pure blue devices [89]. Moreover, the inserted transition layer facilitated hole injection and reduced electron leakage. This improvement in charge balance subsequently contributed to a brightness in QLEDs with PBO that is about 2.6-fold that of the device without PBO under the same current density (Fig. 7h). These factors combined contributed to an enhanced external quantum efficiency (EQE) of 23% (Fig. 7 i).

In summary, the deep VB of blue QDs creates a significant injection barrier that hinders hole transport, making charge-transfer balancing a challenging task in the development of blue QLEDs. High hole mobility and deep HOMO levels are required in the HTL to improve hole injection. A comparison of various HTMs revealed that TFB exhibited low turn-on voltages and high luminance, but low EQE, whereas PVK exhibited high efficiency, but lower maximum luminance and high turn-on voltage. Therefore, combining these HTMs results in high efficiency, low turn-on, and high luminance. Doping HTMs has proven to be an effective approach. Traditional methods of hole injection

improvement face limitations owing to energy level alignment and potential device degradation. Thus, effective strategies such as introducing additional layers of MoO_3 or an anti-oxidation layer to strengthen hole injection and transport are feasible approaches to balance carrier injection for efficient blue InP QLEDs.

Suppressing Excess Electrons

The wide bandgap of blue QDs limits the achievement of charge balance by merely increasing hole injection. Considering the ETL side, suppressing excess electrons while enhancing hole injection can lead to superior charge injection balance. In the initial stages of QLED research, ETL materials typically comprised organic substances, such as Alq_3 , TPBi, BPhen, TNF, and rare earth complexes [93, 94]. However, the low electron mobility of these organic molecules (10^{-6} – $10^{-4} \text{ cm}^2 \text{ V}^{-1} \text{ s}^{-1}$) caused an imbalance between holes and electrons, reducing the device efficiency. Consequently, attention shifted toward metal oxides, such as ZnO, TiO_2 , and SnO_2 , which exhibited higher electron mobilities [95]. In 2009, Cho et al. used TiO_2 with high electron mobility ($1.7 \times 10^{-4} \text{ cm}^2 \text{ V}^{-1} \text{ s}^{-1}$) to effectively inject electrons and holes from the electrodes to the QD layer, improving the device through a small energy barrier of just 0.4 eV. In 2011, Lei et al. fabricated a significantly improved blue QLED using high electron mobility ZnO nanoparticles (NPs), achieving maximum luminance and power efficiency of 4200 cd m^{-2} and 0.17 lm W^{-1} , respectively [58]. In 2013, Mashford et al. controlled the distance of the recombination region within the QD film at the QD/ZnO interface, reaching a current efficiency of 19 cd A^{-1} and an EQE close to the theoretical peak of 20% at approximately 18% [96]. In 2017, Wang et al. investigated various sizes of ZnO NPs and found that blue QLEDs with smaller ZnO NPs exhibited superior charge balance and high efficiency, with a current efficiency of 14.1 cd A^{-1} and an EQE of 19.8%. [33] However, a certain potential barrier still exists between the blue QD and ZnO layers, especially when compared to red or green. Therefore, ZnO doped with other metal elements (Mg, Al, and Ga) has often been used as an electron transfer material to modify the energy level structure and electron mobility of ZnO, leading to enhanced EL efficiency and stability of the device [97–100]. In 2018, Kim et al. reported the use of Li- and Mg-doped ZnO, MLZO, in the ETL for achieving high-efficiency QLEDs (Fig. 8a). [90] By comparing single devices shown in Fig. 8c, d, co-doping of Mg and Li in ZnO broadens the bandgap and improved the electrical resistivity, leading to enhanced charge balance in the QD EML (Fig. 8d). In addition, a decrease in the OH concentration on the oxide surface and a longer exciton decay time in the QDs on the metal oxide were observed. In the same year, Pan et al. used CsN_3 -doped ZnO NPs as an ETL,

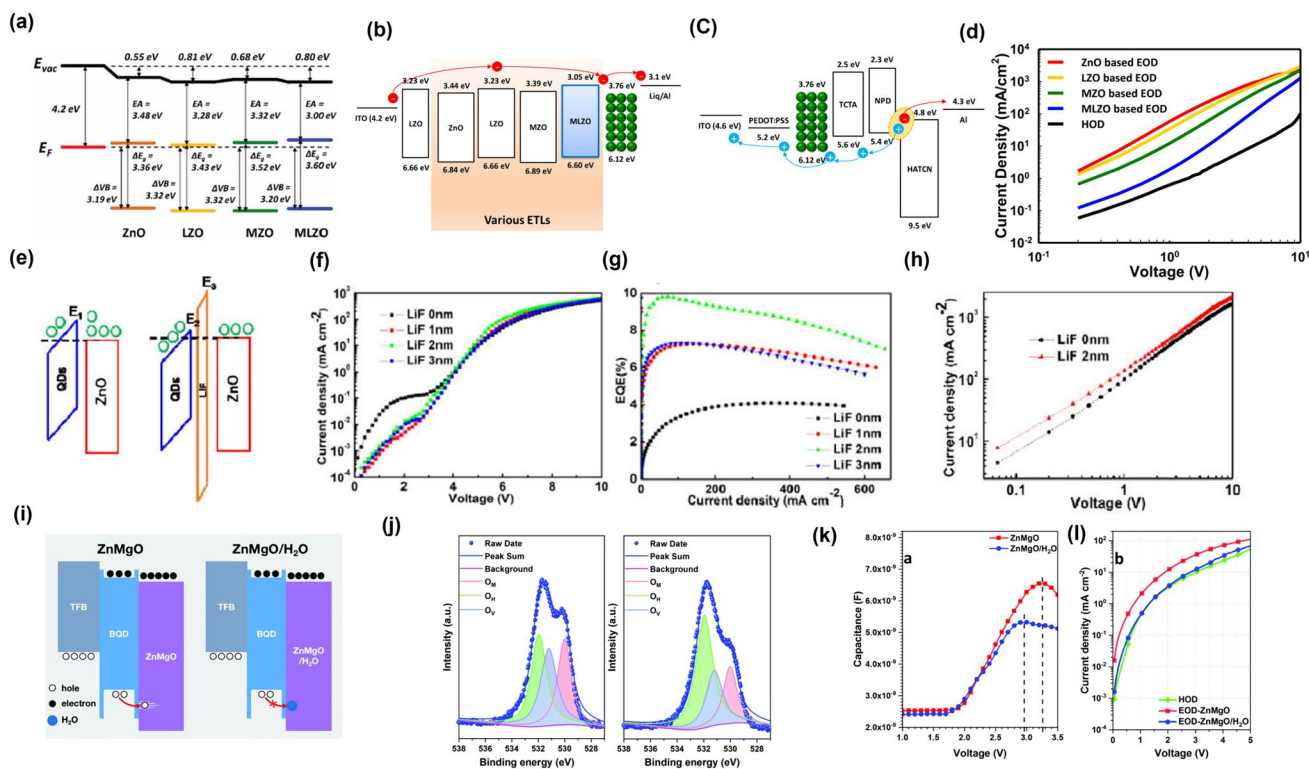


Fig. 8 Characterization and comparative analysis of ETLs in blue QLEDs. **a** Energy band diagram of ITO, ZnO, lithium-doped ZnO (LZO), magnesium-doped ZnO (MZO), and lithium-magnesium co-doped ZnO (MLZO) as ETLs with a doping concentration of 10% for each element. Energy band diagrams of **b** EODs, **c** HODs, and **d** their J–V characteristics. Reproduced with permission. [90] Copyright 2018, American Chemical Society. **e** Schematic of electron tunneling model at the QD/ZnO heterojunction interface. **f** J–V characteristics and **g** EQE of QLEDs. J–V characteristics of EOD with or without

LiF interlayer. Reproduced with permission [91]. Copyright 2019, AIP publishing. **i** Schematic of exciton quenching (left) and restricted exciton quenching (right) at the QD/ZnMgO interface. **j** XPS oxygen (O 1s) spectra of ZnMgO and ZnMgO with surface adsorbed water (H₂O) nanoparticles (NPs). **k** Capacitance–Voltage characteristic of blue QLEDs using ZnMgO and ZnMgO/H₂O ETLs. **l** J–V characteristics of EOD and HOD. Reproduced with permission [92]. Copyright 2021, Royal Society of Chemistry

effectively reducing the excess electron flow and achieving a blue QLED EQE of 6.6% through charge balance [101]. This result was attributed to an increase in the ETL's conduction band maximum of QDs (CBM) edge by 0.27 eV, which suppressed exciton quenching and maintained the excellent emission characteristics of the QDs because of the insulating CsN₃. In 2018, Kai et al. introduced an insulating polymer PVP as an electron-blocking material in the ETL and separated the ZnO NPs, reducing electron injection and achieving charge balance in the blue QLED emitting layer [102]. This method allowed the device to reach a maximum luminance of 22,800 cd m⁻² and an EQE of 2.95%.

In 2019, a simple and effective method for optimizing the performance of blue QLEDs was discovered that involved the use of hybrid charge transport layers [103]. The hybrid HTL composed of TCTA and TFB combined the advantages of high hole mobility and a reduced hole injection barrier, effectively promoting hole injection efficiency. On the cathode side, they modify Al-doped ZnO with zirconium acetylacetonate to reduce the electron transfer within

the ETL, which suppressed the excess electron current. Consequently, a significant increase in the luminance and EQE from 18,679 to 34,874 cd m⁻² and 4.7% to 10.7%, respectively, was observed. In addition, the more balanced charges led to a reduction in QD charge, non-radiative Auger recombination, and leakage current to the HTLs, improving the operating life of the blue QLEDs by approximately 3.5 times. In 2021, ETL doping led to a dramatic increase in maximum EQE and luminance to 7.3% and 9108 cd m⁻², respectively, by tuning the energy levels and carrier mobility in the ETL to result in more balanced charge injection, transport, and recombination in blue QLEDs [104].

Introducing an additional layer is also an effective method for improving charge injection and balance. In 2015, the polyethyleneimine ethoxylated (PEIE) layer was introduced as EIL/ETL to bond with the colloidal ZnO NP film on the ITO electrode [105]. PEIE helped to reduce the work function of ZnO from 3.58 to 2.87 eV, facilitating electron injection into the QDs and maintaining charge balance in the EML. Consequently, the device exhibited low turn-on voltages of

2.0–2.5V, with a maximum luminance of 8,600 cd m^{-2} and a current efficiency of 1.53 cd A^{-1} . In 2017, Liao et al. reduced the electron-transport barrier at the interface from 0.7 to 0.4 eV through PEIE/ZnO, and integrating PEIE into the ZnO layer reduced the electron injection barrier from 0.5 to 0.1 eV [106]. These two interface modifications reduce the electron barrier and made electron transport easier, improving exciton recombination in the QD layer and enhancing device efficiency, resulting in a 1.4 times improvement to an EQE of 7.85%. In 2019, Chen et al. inserted a lithium fluoride (LiF) interlayer between the QD and ZnO layers to enhance the device efficiency and stability of blue QLEDs (Fig. 8e) [91]. The LiF interlayer facilitated electron injection into the QDs through electron tunneling effect and simultaneously suppressed exciton quenching at the QD/ZnO interface. The blue QLED devices exhibit a maximum EQE of 9.8% and a current efficiency of 7.9 cd A^{-1} (Fig. 8f, g, h). In the same year, Li et al. used TBS-PBO as a blocking layer, which prevented excess electron injection and preserved the QD PLQY efficiency, resulting in improved charge-transfer balance [107]. TBS-PBO exhibited superior conductivity than the insulating blocking layers, enabling a higher level of current density, resulting in a blue QLED exhibiting an EQE of 17.4% and a maximum luminance of 4635 cd m^{-2} . TRPL measurements indicated that PL quenching was negligible with the TBS-PBO layer, suggesting preservation of the emission capability of QD emitter.

The performance of QLEDs, particularly blue QLEDs, is significantly affected by exciton quenching and unbalanced charge carriers. To address this issue, passivation of the ETL has also been suggested as a potential solution. In 2021, water was used as a passivation agent to anchor the interface between QDs and ZnMgO, with oxygen atoms filling oxygen vacancies on the ZnMgO surface through electrostatic interaction, reducing surface defects and enabling reduced quenching by excitons formed inside the QDs (Fig. 8i, j) [92]. Conversely, a slight reduction in electron transport from ZnMgO to QDs balances the holes and electrons within the QD emitting layer (Fig. 8k, l). Consequently, blue QLEDs manufactured with water-passivated ZnMgO exhibited an improved external quantum efficiency (EQE) of 11% at 6 V and a luminance exceeding 20,000 cd m^{-2} . In the same year, Xiangwei et al. used chlorine-passivated ZnO NPs as an ETL to effectively promote electron injection into QDs, blocking the charge-transfer channel and suppressing exciton quenching at the QD/ZnO interface [108]. Consequently, the maximum external quantum efficiency of blue QLEDs increased from 2.55 to 4.60%, and the operating life of blue QLEDs was reported to be almost four times longer than that of control devices. In 2019, Tai et al. conducted a study to explore the potential of ZnO NPs and Al:Al₂O₃ as ETL and cathode materials, respectively, for high-performance QLEDs. This study investigated the effects of

post-annealing temperature on the trap state density in ZnO NP and the related mechanisms [109]. By controlling the annealing temperature of ZnO NPs, researchers were able to optimize the charge injection balance and achieve tunable electron mobility in the ETL. The partially oxidized Al cathode (Al:Al₂O₃) contributed to the high-performance blue QLED with a maximum luminance of 27,753 cd m^{-2} and an EQE of 8.92%.

Further Issues in Blue QLEDs: Operational Lifetime

Blue QLEDs, with a lifetime of around 32,705 h, still fall short of commercial standards (refer to Fig. 9 [116]). As illustrated in Fig. 9, a comparative analysis of the lifetimes of blue QLEDs and blue OLEDs has been conducted. OLEDs demonstrate considerably longer lifetimes, and the T_{50} at the initial luminance of 1000 cd m^{-2} can be adjusted to T_{50} of initial luminance of 100 cd m^{-2} through the equation $L_0^n \times T = \text{constant}$, where acceleration factor $n = 1.7$ was applied to the equation [111]. This comparison highlights that, despite recent improvements, blue QLEDs still fall short, with their lifetimes being significantly deficient in comparison to blue OLEDs. Table 2 shows the summarized lifetimes of blue OLEDs and QLEDs.

Similar to efficiency, the relatively rapid degradation of blue QLEDs is primarily attributed to the energy mismatch between the VB of blue QDs and the HOMO level of the HTL. This mismatch leads to a high hole injection barrier, hindering the flow of holes, resulting in severe charge imbalance and the formation of numerous excitons within the organic HTL due to excess electrons. These excitons can induce HTL degradation, causing Auger recombination and joule heating, which collectively can lead to reduced performance and operational lifetime of the QLEDs [121–123].

Enhancing the lifetime of blue QLEDs has been achieved through a combination of advanced material and structural modifications. Initially, blue QLEDs with Zn_xCd_{1-x}S/ZnS structures exhibited lifetimes ranging from several hours to tens of hours. Introducing a thin ZnS outer shell improved this to about 1000 h by enhancing charge injection and suppressing non-radiative recombination. Replacing traditional ligands with electrochemically inert fatty amine ligands in CdSeS/ZnSeS/ZnS QDs significantly bridged the photoluminescence-electroluminescence gap, resulting in lifetimes of 10,000 h at 62,600 cd/m^2 brightness. Enlarging core sizes and adding intermediate shells in large-core ZnCdSe/ZnSeS/ZnCdS/ZnS QDs reduced surface-bulk coupling, achieving lifetimes of 80,377 h. The synthesis of InP/ZnS QDs with optimized core/shell structures addressed lattice mismatches, yielding over 1000 h of lifetime. ZnTeSe QDs,

Fig. 9 Lifetime comparison of current blue OLEDs and blue QLEDs over years. The graph depicts the operational lifetime (T_{50}) of blue OLED (in red) [110], Cd-based blue QLED (dark blue), and Cd-free blue QLED (light blue), measured at 100 cd m^{-2} . The dashed lines represent the lifetime trend for each device type, suggesting extrapolation beyond the measured data. T_{50} of OLEDs are converted from the original data (T_{50} at an initial luminance of 1000 cd m^{-2}) using the equation $L_0^n \times T = \text{constant}$, with an acceleration factor of $n = 1.7$ [111–115]

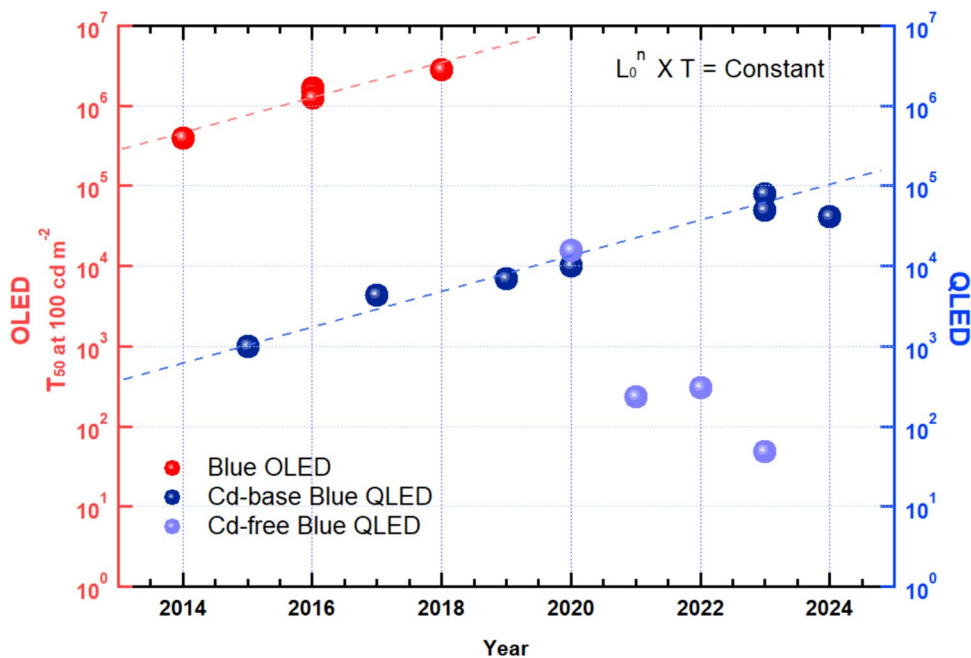


Table 2 Summary of blue OLED and QLED lifetime

Year	Core material	Initial luminance [cd m^{-2}] / T_{50} [h]	Calculated T_{50} [h]	Acceleration factor [n]	References
OLED					
2014	–	1000/8000	400,950	1.70	[110, 117]
2016	–	1000/14,000	1,252,968	1.70	[110, 117]
2016	–	1000/30,000	1,503,562	1.70	[110, 117]
2016	–	1000/33,902	1,699,125	1.70	[110, 117]
2018	–	1000/56,000	2,806,649	1.70	[110, 117]
Cd-base QLED					
2015	CdZnS	–	1,000	1.96	[21]
2017	ZnCdS	420/47 (T_{70})	–	–	[118]
2019	ZnCdSe	7000/6	7,000	1.64	[119]
2020	CdSeS	1450.85	10,000	1.88	[59]
2023	ZnCdSe	1000/151 (T_{95})	50,206	1.80	[34]
2023	ZnCdSe	1000/227 (T_{95})	80,377	1.79	[34]
2024	CdZnS	3914/60	41,022	1.78	[89]
Cd-free QLED					
2020	ZnTeSe	650/442	15,850	1.9	[74]
2021	ZnSe	570/~27	237	–	[47]
2022	ZnSe	–	305	–	[120]
2023	ZnTeSe	1023/~0.76	49.1	1.8	[48]

enhanced with HF and ZnCl_2 additives, achieved lifetimes of 15,850 h at $88,900 \text{ cd/m}^2$ brightness by improving ligand separation and shell growth direction. In addition, alloying ZnSe with ZnTe to create ZnSeTe/ZnSe/ZnS QDs effectively adjusted the bandgap, leading to lifetimes exceeding 10,000 h. These comprehensive strategies have

significantly advanced the durability and performance of blue-emitting QLEDs.

However, Chen et al. found that while HTL degradation occurs in both red and blue QLEDs, it does not explain the shorter lifetime of blue QLEDs [124]. They then observed that rapid degradation is associated with an increase in

capacitance transition voltage in blue QLEDs. Upon a thorough investigation of charge-modulated electro-absorption and capacitance–voltage characteristics, they discovered that it was not the hole injection barrier due to the difference in VB and HOMO levels of blue QDs and HTLs but rather the large offset between the CBM and ETL that leads to space charge accumulation and an increase in the operating voltage of the ETL. Therefore, unlike stable red QLEDs ($T_{50} > 800$ h), where the lifetime is primarily derived from the slow degradation of the HTL, the inferior lifetime of blue QLEDs ($T_{50} < 4.5$ h) is mainly due to Auger recombination and rapid degradation at the QD/ETL interface. In essence, while in QLEDs, the HTL generally degrades over time and contributes to device aging, in blue QLEDs, the core of the performance degradation lies in the dynamics at the QD–ETL interface. Thus, addressing the lifetime issues of blue QLEDs will require the development of ETL and QD materials that enable smaller CBM offsets.

Conclusion

In conclusion, blue QDs are limited in lifetime and efficiency due to various issues such as deep VB minimum, wide band-gap, surface defects, and so on. To address these issues, various methods have been introduced, and the performance of QLEDs using Cd-based QDs has been greatly improved. However, environmental concerns due to the toxicity of cadmium limit their use. Also, blue QDs show size-dependent color emission, but smaller QDs necessary for blue emission complicate the manufacturing process. Consequently, achieving high efficiency while maintaining a narrow emission spectrum using eco-friendly materials is challenging. The development and optimization of environmentally friendly alternatives such as InP or ZnSe Cd-free materials are required, and QLEDs using ZnSe-based ZnTeSe QDs exhibited very high performance. This can address toxicity issues while maintaining efficiency and stability. Furthermore, blue QLEDs can be affected by charge injection imbalance between QDs and the HTL and ETL; this can negatively affect the device's efficiency and lifetime. The mismatch in the energy levels between the current materials hinders efficient charge transfer, which is a crucial issue in blue QLEDs. Therefore, it is essential to develop new HTL and ETL materials that provide appropriate energy levels while featuring high hole and electron mobilities. In addition, optimization of the interfaces between the QDs and the adjacent layers is required to reduce the charge injection barriers and prevent exciton quenching. Strategies to extend the lifetime of blue QLEDs through material and structural optimization, interface passivation, and improved thermal stability are required. In this study, we reviewed the overall issues, challenges, and progress of blue QDs and their

application in blue QLED. We hope that this research could contribute to the commercialization of blue QLEDs.

Acknowledgements This work was supported by the Basic Science Research Program (NRF-2022R1F1A1066526) through the National Research Foundation of the Ministry of Education, Republic of Korea. This research (for Hyunho Lee) was partially supported by Basic Science Research Program through the National Research Foundation of Korea (NRF) funded by the Ministry of Education (No. 2018R1A6A1A03025242). The present research has been conducted by the Excellent researcher support project of Kwangwoon University in 2024.

Data availability This article does not produce or analyze new data. All data referenced in this article come from previously published sources, which are duly cited throughout the manuscript. Therefore, data availability is not applicable to this article.

References

1. K. Kim, M. Kim, J. Yang, Recent developments in quantum dot light-emitting diodes for skin-attachable electronics Korean J. Chem. Eng. (2024). <https://doi.org/10.1007/s11814-024-00179-1>
2. J. Fan, C. Han, G. Yang, B. Song, R. Xu, C. Xiang, T. Zhang, L. Qian, Recent progress of quantum dots light-emitting diodes: materials, device structures, and display applications. Adv. Mater. **n/a**, 2312948 (2024)
3. G.D. Cha, D.-H. Kim, D.C. Kim, Wearable and implantable light-emitting diodes and their biomedical applications. Korean J. Chem. Eng. **41**, 1–24 (2024)
4. C. Murray, D.J. Norris, M.G. Bawendi, Synthesis and characterization of nearly monodisperse CdE (E = sulfur, selenium, tellurium) semiconductor nanocrystallites. J. Am. Chem. Soc. **115**(19), 8706–8715 (1993)
5. S. Coe, W.-K. Woo, M. Bawendi, V. Bulović, Electroluminescence from single monolayers of nanocrystals in molecular organic devices. Nature **420**(6917), 800–803 (2002)
6. K.-S. Cho, E.K. Lee, W.-J. Joo, E. Jang, T.-H. Kim, S.J. Lee, S.-J. Kwon, J.Y. Han, B.-K. Kim, B.L. Choi, J.M. Kim, High-performance crosslinked colloidal quantum-dot light-emitting diodes. Nat. Photonics **3**(6), 341–345 (2009)
7. Q. Sun, Y.A. Wang, L.S. Li, D. Wang, T. Zhu, J. Xu, C. Yang, Y. Li, Bright, multicoloured light-emitting diodes based on quantum dots. Nat. Photonics **1**(12), 717–722 (2007)
8. W. Cao, C. Xiang, Y. Yang, Q. Chen, L. Chen, X. Yan, L. Qian, Highly stable QLEDs with improved hole injection via quantum dot structure tailoring. Nat. Commun. **9**(1), 2608 (2018)
9. G. Rajapriya, R. Sangubotla, J. Kim, Synthesis of a fluorescent sensor by exploiting nitrogen-doped MXene quantum dots for the detection of dopamine. Korean J. Chem. Eng. (2024). <https://doi.org/10.1007/s11814-024-00144-y>
10. Z. Chen, H. Li, C. Yuan, P. Gao, Q. Su, S. Chen, Color revolution: prospects and challenges of quantum-dot light-emitting diode display technologies. Small Methods **8**(2), 2300359 (2024)
11. Z. Yang, M. Gao, W. Wu, X. Yang, X.W. Sun, J. Zhang, H.-C. Wang, R.-S. Liu, C.-Y. Han, H. Yang, Recent advances in quantum dot-based light-emitting devices: challenges and possible solutions. Mater. Today **24**, 69–93 (2019)
12. Y. Shirasaki, G.J. Supran, M.G. Bawendi, V. Bulović, Emergence of colloidal quantum-dot light-emitting technologies. Nat. Photonics **7**(1), 13–23 (2013)

13. E. Jang, H. Jang, Review: quantum dot light-emitting diodes. *Chem. Rev.* **123**(8), 4663–4692 (2023)
14. K.-H. Lee, J.-H. Lee, H.-D. Kang, B. Park, Y. Kwon, H. Ko, C. Lee, J. Lee, H. Yang, Over 40 cd/A efficient green quantum dot electroluminescent device comprising uniquely large-sized quantum dots. *ACS Nano* **8**(5), 4893–4901 (2014)
15. J. Lim, B.G. Jeong, M. Park, J.K. Kim, J.M. Pietryga, Y.S. Park, V.I. Klimov, C. Lee, D.C. Lee, W.K. Bae, Influence of shell thickness on the performance of light-emitting devices based on CdSe/Zn1-XCdXS core/shell heterostructured quantum dots. *Adv. Mater.* **26**(47), 8034–8040 (2014)
16. B.N. Pal, Y. Ghosh, S. Brovelli, R. Laocharoensuk, V.I. Klimov, J.A. Hollingsworth, H. Htoon, ‘Giant’ CdSe/CdS core/shell nanocrystal quantum dots as efficient electroluminescent materials: strong influence of shell thickness on light-emitting diode performance. *Nano Lett.* **12**(1), 331–336 (2012)
17. E. Mutlugun, B. Guzelturk, A.P. Abiyasa, Y. Gao, X.W. Sun, H.V. Demir, Colloidal quantum dot light-emitting diodes employing phosphorescent small organic molecules as efficient exciton harvesters. *J. Phys. Chem. Lett.* **5**(16), 2802–2807 (2014)
18. X. Yang, Y. Ma, E. Mutlugun, Y. Zhao, K.S. Leck, S.T. Tan, H.V. Demir, Q. Zhang, H. Du, X.W. Sun, Stable, efficient, and all-solution-processed quantum dot light-emitting diodes with double-sided metal oxide nanoparticle charge transport layers. *ACS Appl. Mater. Interfaces* **6**(1), 495–499 (2014)
19. X. Dai, Z. Zhang, Y. Jin, Y. Niu, H. Cao, X. Liang, L. Chen, J. Wang, X. Peng, Solution-processed, high-performance light-emitting diodes based on quantum dots. *Nature* **515**(7525), 96–99 (2014)
20. C. Lee, W. Bae, J. Kwak 차세대 디스플레이 기술로 부상하는 양자점 발광 다이오드. *Mater. Sci.* **30** 5452000
21. Y. Yang, Y. Zheng, W. Cao, A. Titov, J. Hyvonen, J.R. Manders, J. Xue, P.H. Holloway, L. Qian, High-efficiency light-emitting devices based on quantum dots with tailored nanostructures. *Nat. Photonics* **9**(4), 259–266 (2015)
22. C. Luo, Z. Zheng, Y. Ding, Z. Ren, H. Shi, H. Ji, X. Zhou, Y. Chen, High-resolution, highly transparent, and efficient quantum dot light-emitting diodes. *Adv. Mater.* **35**(33), 2303329 (2023)
23. H. Park, C. Na, H. Lee, S.M. Cho, A top-down fabrication process for a-IGZO thin film transistor and patterned organic light-emitting diode. *Korean J. Chem. Eng.* **40**(3), 667–674 (2023)
24. H. Shen, Q. Gao, Y. Zhang, Y. Lin, Q. Lin, Z. Li, L. Chen, Z. Zeng, X. Li, Y. Jia, S. Wang, Z. Du, L.S. Li, Z. Zhang, Visible quantum dot light-emitting diodes with simultaneous high brightness and efficiency. *Nat. Photonics* **13**(3), 192–197 (2019)
25. X. Dai, Y. Deng, X. Peng, Y. Jin, Quantum-dot light-emitting diodes for large-area displays: towards the dawn of commercialization. *Adv. Mater.* **29**(14), 1607022 (2017)
26. Y. Sun, Y. Jiang, X.W. Sun, S. Zhang, S. Chen, Beyond OLED: efficient quantum dot light-emitting diodes for display and lighting application. *Chem. Rec.* **19**(8), 1729–1752 (2019)
27. Y. Liu, C. Jiang, C. Song, J. Wang, L. Mu, Z. He, Z. Zhong, Y. Cun, C. Mai, J. Wang, J. Peng, Y. Cao, Highly efficient all-solution processed inverted quantum dots based light emitting diodes. *ACS Nano* **12**(2), 1564–1570 (2018)
28. L. Wang, J. Lin, Y. Lv, B. Zou, J. Zhao, X. Liu, Red, green, and blue microcavity quantum dot light-emitting devices with narrow line widths. *ACS Appl. Nano Mater.* **3**(6), 5301–5310 (2020)
29. Y. Deng, F. Peng, Y. Lu, X. Zhu, W. Jin, J. Qiu, J. Dong, Y. Hao, D. Di, Y. Gao, T. Sun, M. Zhang, F. Liu, L. Wang, L. Ying, F. Huang, Y. Jin, Solution-processed green and blue quantum-dot light-emitting diodes with eliminated charge leakage. *Nat. Photonics* **16**(7), 505–511 (2022)
30. J. Kim, J. Roh, M. Park, C. Lee, Recent advances and challenges of colloidal quantum dot light-emitting diodes for display applications. *Adv. Mater.* **36**, 2212220 (2024)
31. T. Lee, B.J. Kim, H. Lee, D. Hahm, W.K. Bae, J. Lim, J. Kwak, Bright and stable quantum dot light-emitting diodes. *Adv. Mater.* **34**(4), 2106276 (2022)
32. O. Wang, L. Wang, Z. Li, Q. Xu, Q. Lin, H. Wang, Z. Du, H. Shen, L.S. Li, High-efficiency, deep blue ZnCdS/Cd x Zn 1-x S/ ZnS quantum-dot-light-emitting devices with an EQE exceeding 18%. *Nanoscale* **10**(12), 5650–5657 (2018)
33. L. Wang, J. Lin, Y. Hu, X. Guo, Y. Lv, Z. Tang, J. Zhao, Y. Fan, N. Zhang, Y. Wang, Blue quantum dot light-emitting diodes with high electroluminescent efficiency. *ACS Appl. Mater. Interfaces* **9**(44), 38755–38760 (2017)
34. X. Chen, X. Lin, L. Zhou, X. Sun, R. Li, M. Chen, Y. Yang, W. Hou, L. Wu, W. Cao, X. Zhang, X. Yan, S. Chen, Blue light-emitting diodes based on colloidal quantum dots with reduced surface-bulk coupling. *Nat. Commun.* **14**(1), 284 (2023)
35. A. Laaperi, OLED lifetime issues from a mobile-phone-industry point of view. *J. Soc. Inf. Disp.* **16**(11), 1125–1130 (2008)
36. D. Tian, H. Ma, G. Huang, M. Gao, F. Cai, Y. Fang, C. Li, X. Jiang, A. Wang, S. Wang, Z. Du, A review on quantum dot light-emitting diodes: from materials to applications. *Adv. Opt. Mater.* **11**(2), 2201965 (2023)
37. H. Jia, F. Wang, Z. Tan, Material and device engineering for high-performance blue quantum dot light-emitting diodes. *Nanoscale* **12**(25), 13186–13224 (2020)
38. H. Qi, S. Wang, X. Jiang, Y. Fang, A. Wang, H. Shen, Z. Du, Research progress and challenges of blue light-emitting diodes based on II–VI semiconductor quantum dots. *J. Mater. Chem. C* **8**(30), 10160–10173 (2020)
39. M.A. Hines, P. Guyot-Sionnest, Synthesis and characterization of strongly luminescing ZnS-capped CdSe nanocrystals. *J. Phys. Chem.* **100**(2), 468–471 (1996)
40. X. Peng, M.C. Schlamp, A.V. Kadavanich, A.P. Alivisatos, Epitaxial growth of highly luminescent CdSe/CdS core/shell nanocrystals with photostability and electronic accessibility. *J. Am. Chem. Soc.* **119**(30), 7019–7029 (1997)
41. T. Takagahara, K. Takeda, Theory of the quantum confinement effect on excitons in quantum dots of indirect-gap materials. *Phys. Rev. B* **46**(23), 15578 (1992)
42. P. Reiss, M. Carriere, C. Lincheneau, L. Vaure, S. Tamang, Synthesis of semiconductor nanocrystals, focusing on nontoxic and earth-abundant materials. *Chem. Rev.* **116**(18), 10731–10819 (2016)
43. L. Chen, Z. Qin, S. Chen, Ultrahigh resolution pixelated top-emitting quantum-dot light-emitting diodes enabled by color-converting cavities. *Small Methods* **6**(1), 2101090 (2022)
44. Y. Tan, W. Zhang, X. Xiao, J. Sun, J. Ma, T. Zhang, G. Mei, Z. Wang, F. Zhao, D. Wu, Enhancing hole injection by electric dipoles for efficient blue InP QLEDs. *Appl. Phys. Lett.* (2021). <https://doi.org/10.1063/5.0071508>
45. P. Gao, Y. Zhang, P. Qi, S. Chen, Efficient InP green quantum-dot light-emitting diodes based on organic electron transport layer. *Adv. Opt. Mater.* **10**(24), 2202066 (2022)
46. Q. Su, H. Zhang, S. Chen, Identification of excess charge carriers in InP-based quantum-dot light-emitting diodes. *Appl. Phys. Lett.* (2020). <https://doi.org/10.1063/5.0019790>
47. M. Gao, H. Yang, H. Shen, Z. Zeng, F. Fan, B. Tang, J. Min, Y. Zhang, Q. Hua, L.S. Li, Bulk-like ZnSe quantum dots enabling efficient ultranarrow blue light-emitting diodes. *Nano Lett.* **21**(17), 7252–7260 (2021)
48. Y. Bi, S. Cao, P. Yu, Z. Du, Y. Wang, J. Zheng, B. Zou, J. Zhao, Reducing emission linewidth of pure-blue ZnSeTe quantum dots through shell engineering toward high color purity light-emitting diodes. *Small* **19**(45), 2303247 (2023)

49. J. Kim, J. Roh, M. Park, C. Lee, Recent advances and challenges of colloidal quantum dot light-emitting diodes for display applications. *Adv. Mater.* **36**, 2212220 (2023)
50. H.-V. Han, H.-Y. Lin, C.-C. Lin, W.-C. Chong, J.-R. Li, K.-J. Chen, P. Yu, T.-M. Chen, H.-M. Chen, K.-M. Lau, H.-C. Kuo, Resonant-enhanced full-color emission of quantum-dot-based micro LED display technology. *Opt. Express* **23**(25), 32504–32515 (2015)
51. Y. Shirasaki, G.J. Supran, W.A. Tisdale, V. Bulović, Origin of efficiency roll-off in colloidal quantum-dot light-emitting diodes. *Phys. Rev. Lett.* **110**(21), 217403 (2013)
52. D. Bozyigit, O. Yarema, V. Wood, Origins of low quantum efficiencies in quantum dot LEDs. *Adv. Funct. Mater.* **23**(24), 3024–3029 (2013)
53. M.L. Steigerwald, A.P. Alivisatos, J. Gibson, T. Harris, R. Kortan, A. Muller, A. Thayer, T. Duncan, D. Douglass, L.E. Brus, Surface derivatization and isolation of semiconductor cluster molecules. *J. Am. Chem. Soc.* **110**(10), 3046–3050 (1988)
54. O. Chen, J. Zhao, V.P. Chauhan, J. Cui, C. Wong, D.K. Harris, H. Wei, H.-S. Han, D. Fukumura, R.K. Jain, Compact high-quality CdSe–CdS core–shell nanocrystals with narrow emission linewidths and suppressed blinking. *Nat. Mater.* **12**(5), 445–451 (2013)
55. H. Shen, X. Bai, A. Wang, H. Wang, L. Qian, Y. Yang, A. Titov, J. Hyvonen, Y. Zheng, L.S. Li, High-efficient deep-blue light-emitting diodes by using high quality Zn_xCd_{1-x}S/ZnS core/shell quantum dots. *Adv. Funct. Mater.* **24**(16), 2367–2373 (2014)
56. H. Shen, W. Cao, N.T. Shewmon, C. Yang, L.S. Li, J. Xue, High-efficiency, low turn-on voltage blue-violet quantum-dot-based light-emitting diodes. *Nano Lett.* **15**(2), 1211–1216 (2015)
57. W.K. Bae, J. Kwak, J. Lim, D. Lee, M.K. Nam, K. Char, C. Lee, S. Lee, Deep blue light-emitting diodes based on Cd_{1-x}Zn_xS@ZnS quantum dots. *Nanotechnology* **20**(7), 075202 (2009)
58. L. Qian, Y. Zheng, J. Xue, P.H. Holloway, Stable and efficient quantum-dot light-emitting diodes based on solution-processed multilayer structures. *Nat. Photonics* **5**(9), 543–548 (2011)
59. C. Pu, X. Dai, Y. Shu, M. Zhu, Y. Deng, Y. Jin, X. Peng, Electrochemically-stable ligands bridge the photoluminescence-electroluminescence gap of quantum dots. *Nat. Commun.* **11**(1), 937 (2020)
60. S.-N. Li, J.-L. Pan, Y.-J. Yu, F. Zhao, Y.-K. Wang, L.-S. Liao, Advances in solution-processed blue quantum dot light-emitting diodes. *Nanomaterials* **13**(10), 1695 (2023)
61. W. Zhang, S. Ding, W. Zhuang, D. Wu, P. Liu, X. Qu, H. Liu, H. Yang, Z. Wu, K. Wang, InP/ZnS/ZnS core/shell blue quantum dots for efficient light-emitting diodes. *Adv. Funct. Mater.* **30**(49), 2005303 (2020)
62. H. Zhang, X. Ma, Q. Lin, Z. Zeng, H. Wang, L.S. Li, H. Shen, Y. Jia, Z. Du, High-brightness blue InP quantum dot-based electroluminescent devices: the role of shell thickness. *J. Phys. Chem. Lett.* **11**(3), 960–967 (2020)
63. K.-H. Kim, J.-H. Jo, D.-Y. Jo, C.-Y. Han, S.-Y. Yoon, Y. Kim, Y.-H. Kim, Y.H. Ko, S.W. Kim, C. Lee, H. Yang, Cation-exchange-derived InGaP alloy quantum dots toward blue emissivity. *Chem. Mater.* **32**(8), 3537–3544 (2020)
64. M. Gao, H. Yang, H. Shen, Z. Zeng, F. Fan, B. Tang, J. Min, Y. Zhang, Q. Hua, L.S. Li, B. Ji, Z. Du, Bulk-like ZnSe quantum dots enabling efficient ultranarrow blue light-emitting diodes. *Nano Lett.* **21**(17), 7252–7260 (2021)
65. W. Shen, H. Tang, X. Yang, Z. Cao, T. Cheng, X. Wang, Z. Tan, J. You, Z. Deng, Synthesis of highly fluorescent InP/ZnS small-core/thick-shell tetrahedral-shaped quantum dots for blue light-emitting diodes. *J. Mater. Chem. C* **5**(32), 8243–8249 (2017)
66. Y.-H. Kim, S.-Y. Yoon, H. Yang, Blue-emissive ZnSeTe quantum dots and their electroluminescent devices. *J. Phys. Chem. Lett.* **15**(8), 2142–2151 (2024)
67. G. Mei, Y. Tan, J. Sun, D. Wu, T. Zhang, H. Liu, P. Liu, X.W. Sun, W.C. Choy, K. Wang, Light extraction employing optical tunneling in blue InP quantum dot light-emitting diodes. *Appl. Phys. Lett.* (2022). <https://doi.org/10.1063/5.0084416>
68. S. Dey, S. Nath, Electroluminescence of colloidal ZnSe quantum dots. *J. Lumin.* **131**(12), 2707–2710 (2011)
69. W. Ji, P. Jing, Y. Fan, J. Zhao, Y. Wang, X. Kong, Cadmium-free quantum dot light emitting devices: energy-transfer realizing pure blue emission. *Opt. Lett.* **38**(1), 7–9 (2013)
70. C. Xiang, W. Koo, S. Chen, F. So, X. Liu, X. Kong, Y. Wang, Solution processed multilayer cadmium-free blue/violet emitting quantum dots light emitting diodes. *Appl. Phys. Lett.* **101**(5), 053303 (2012)
71. A. Wang, H. Shen, S. Zang, Q. Lin, H. Wang, L. Qian, J. Niu, L.S. Li, Bright, efficient, and color-stable violet ZnSe-based quantum dot light-emitting diodes. *Nanoscale* **7**(7), 2951–2959 (2015)
72. X. Deng, F. Zhang, Y. Zhang, H. Shen, Heavy-metal-free blue-emitting ZnSe (Te) quantum dots: synthesis and light-emitting applications. *J. Mater. Chem. C* **11**(42), 14495–14514 (2023)
73. E.-P. Jang, C.-Y. Han, S.-W. Lim, J.-H. Jo, D.-Y. Jo, S.-H. Lee, S.-Y. Yoon, H. Yang, Synthesis of alloyed ZnSeTe quantum dots as bright, color-pure blue emitters. *ACS Appl. Mater. Interfaces* **11**(49), 46062–46069 (2019)
74. T. Kim, K.-H. Kim, S. Kim, S.-M. Choi, H. Jang, H.-K. Seo, H. Lee, D.-Y. Chung, E. Jang, Efficient and stable blue quantum dot light-emitting diode. *Nature* **586**(7829), 385–389 (2020)
75. S.-H. Lee, S.-W. Song, S.-Y. Yoon, D.-Y. Jo, S.-K. Kim, H.-M. Kim, Y. Kim, S.M. Park, H. Yang, Heterostructural tailoring of blue ZnSeTe quantum dots toward high-color purity and high-efficiency electroluminescence. *J. Chem. Eng.* **429**, 132464 (2022)
76. K.-H. Lee, J.-H. Lee, W.-S. Song, H. Ko, C. Lee, J.-H. Lee, H. Yang, Highly efficient, color-pure, color-stable blue quantum dot light-emitting devices. *ACS Nano* **7**(8), 7295–7302 (2013)
77. M.D. Ho, D. Kim, N. Kim, S.M. Cho, H. Chae, Polymer and small molecule mixture for organic hole transport layers in quantum dot light-emitting diodes. *ACS Appl. Mater. Interfaces* **5**(23), 12369–12374 (2013)
78. D.-H. Lee, Y.-P. Liu, K.-H. Lee, H. Chae, S.M. Cho, Effect of hole transporting materials in phosphorescent white polymer light-emitting diodes. *Org. Electron.* **11**(3), 427–433 (2010)
79. M.W. Thesen, B. Höfer, M. Debeaux, S. Janietz, A. Wedel, A. Köhler, H.H. Johannes, H. Krueger, Hole-transporting host-polymer series consisting of triphenylamine basic structures for phosphorescent polymer light-emitting diodes. *J. Polym. Sci., Part A: Polym. Chem.* **48**(15), 3417–3430 (2010)
80. Y. Tao, C. Yang, J. Qin, Organic host materials for phosphorescent organic light-emitting diodes. *Chem. Soc. Rev.* **40**(5), 2943–2970 (2011)
81. J. Kwak, W.K. Bae, D. Lee, I. Park, J. Lim, M. Park, H. Cho, H. Woo, D.Y. Yoon, K. Char, Bright and efficient full-color colloidal quantum dot light-emitting diodes using an inverted device structure. *Nano Lett.* **12**(5), 2362–2366 (2012)
82. J. Chen, D. Song, S. Zhao, B. Qiao, W. Zheng, Z. Xu, Highly efficient all-solution processed blue quantum dot light-emitting diodes based on balanced charge injection achieved by double hole transport layers. *Org. Electron.* **94**, 106169 (2021)
83. L. Zheng, G. Zhai, Y. Zhang, X. Jin, L. Gao, Z. Yun, Y. Miao, H. Wang, Y. Wu, B. Xu, Solution-processed blue quantum-dot light-emitting diodes based on double hole transport layers: Charge injection balance, solvent erosion control and

- performance improvement. *Superlattices Microstruct.* **140**, 106460 (2020)
84. Q. Lin, H. Shen, H. Wang, A. WanG, J. Niu, L. Qian, F. GuO, L.S. Li, Cadmium-free quantum dots based violet light-emitting diodes: High-efficiency and brightness via optimization of organic hole transport layers. *Org. Electron.* **25**, 178–183 (2015)
 85. L. Wang, T. Chen, Q. Lin, H. Shen, A. Wang, H. Wang, C. Li, L.S. Li, High-performance azure blue quantum dot light-emitting diodes via doping PVK in emitting layer. *Org. Electron.* **37**, 280–286 (2016)
 86. C. Cheng, A. Liu, G. Ba, I.S. Mukhin, F. Huang, R.M. Islamova, W.C. Choy, J. Tian, High-efficiency quantum-dot light-emitting diodes enabled by boosting the hole injection. *J. Mater. Chem. C* **10**(40), 15200–15206 (2022)
 87. X. Huang, S. Su, Q. Su, H. Zhang, F. Wen, S. Chen, The influence of the hole transport layers on the performance of blue and color tunable quantum dot light-emitting diodes. *J. Soc. Inform. Display* **26**(8), 470–476 (2018)
 88. Y. Liu, C. Jiang, C. Song, J. Wang, L. Mu, Z. He, Z. Zhong, Y. Cun, C. Mai, J. Wang, Highly efficient all-solution processed inverted quantum dots based light emitting diodes. *ACS Nano* **12**(2), 1564–1570 (2018)
 89. W. Zhang, B. Li, C. Chang, F. Chen, Q. Zhang, Q. Lin, L. Wang, J. Yan, F. Wang, Y. Chong, Stable and efficient pure blue quantum-dot LEDs enabled by inserting an anti-oxidation layer. *Nat. commun.* **15**(1), 783 (2024)
 90. H.-M. Kim, S. Cho, J. Kim, H. Shin, J. Jang, Li and Mg Codoped zinc oxide electron transporting layer for highly efficient quantum dot light-emitting diodes. *ACS Appl. Mater. Interfaces* **10**(28), 24028–24036 (2018)
 91. X. Qu, N. Zhang, R. Cai, B. Kang, S. Chen, B. Xu, K. Wang, X.W. Sun, Improving blue quantum dot light-emitting diodes by a lithium fluoride interfacial layer. *Appl. Phys. Lett.* (2019). <https://doi.org/10.1063/1.5087102>
 92. Y. Guo, B. Liu, Z. Chen, W. Song, N. Tian, W. Wu, X. Fan, Y. Zhan, F. Meng, Q. Zeng, Water-passivated ZnMgO nanoparticles for blue quantum dot light-emitting diodes. *J. Mater. Chem. C* **9**(32), 10381–10387 (2021)
 93. M.J. Panzer, K.E. Aidala, P.O. Anikeeva, J.E. Halpert, M.G. Bawendi, V. Bulovic, Nanoscale morphology revealed at the interface between colloidal quantum dots and organic semiconductor films. *Nano Lett.* **10**(7), 2421–2426 (2010)
 94. P.O. Anikeeva, J.E. Halpert, M.G. Bawendi, V. Bulovic, Quantum dot light-emitting devices with electroluminescence tunable over the entire visible spectrum. *Nano Lett.* **9**(7), 2532–2536 (2009)
 95. A. Gopal, K. Hoshino, S. Kim, X. Zhang, Multi-color colloidal quantum dot based light emitting diodes micropatterned on silicon hole transporting layers. *Nanotechnology* **20**(23), 235201 (2009)
 96. B.S. Mashford, M. Stevenson, Z. Popovic, C. Hamilton, Z. Zhou, C. Breen, J. Steckel, V. Bulovic, M. Bawendi, S. Coe-Sullivan, High-efficiency quantum-dot light-emitting devices with enhanced charge injection. *Nat. Photonics* **7**(5), 407–412 (2013)
 97. M.-M. Yan, Y. Li, Y.-T. Zhou, L. Liu, Y. Zhang, B.-G. You, Y. Li, Enhancing the performance of blue quantum-dot light-emitting diodes based on Mg-doped ZnO as an electron transport layer. *IEEE Photonics J.* **9**(2), 1–8 (2017)
 98. S. Wang, Y. Guo, D. Feng, L. Chen, Y. Fang, H. Shen, Z. Du, Bandgap tunable Zn 1-x Mg x O thin films as electron transport layers for high performance quantum dot light-emitting diodes. *J. Mater. Chem. C* **5**(19), 4724–4730 (2017)
 99. S. Cao, J. Zheng, J. Zhao, Z. Yang, C. Li, X. Guan, W. Yang, M. Shang, T. Wu, Enhancing the performance of quantum dot light-emitting diodes using room-temperature-processed Ga-doped ZnO nanoparticles as the electron transport layer. *ACS Appl. Mater. Interfaces* **9**(18), 15605–15614 (2017)
 100. J.-H. Kim, C.-Y. Han, K.-H. Lee, K.-S. An, W. Song, J. Kim, M.S. Oh, Y.R. Do, H. Yang, Performance improvement of quantum dot-light-emitting diodes enabled by an alloyed ZnMgO nanoparticle electron transport layer. *Chem. Mater.* **27**(1), 197–204 (2015)
 101. J. Pan, C. Wei, L. Wang, J. Zhuang, Q. Huang, W. Su, Z. Cui, A. Nathan, W. Lei, J. Chen, Boosting the efficiency of inverted quantum dot light-emitting diodes by balancing charge densities and suppressing exciton quenching through band alignment. *Nanoscale* **10**(2), 592–602 (2018)
 102. K. Sun, F. Li, Q. Zeng, H. Hu, T. Guo, Blue quantum dot light emitting diodes with polyvinylpyrrolidone-doped electron transport layer. *Org. Electron.* **63**, 65–70 (2018)
 103. F. Wang, W. Sun, P. Liu, Z. Wang, J. Zhang, J. Wei, Y. Li, T. Hayat, A. Alsaedi, Z. Tan, Achieving balanced charge injection of blue quantum dot light-emitting diodes through transport layer doping strategies. *J. Phys. Chem. Lett.* **10**(5), 960–965 (2019)
 104. Y. Yang, L. Su, N. Feng, A. Liu, X. Xing, M. Lu, W.Y. William, Balanced charge transport and enhanced performance of blue quantum dot light-emitting diodes via electron transport layer doping. *Nanotechnology* **32**(33), 335203 (2021)
 105. H.H. Kim, S. Park, Y. Yi, D.I. Son, C. Park, D.K. Hwang, W.K. Choi, Inverted quantum dot light emitting diodes using polyethyleneimine ethoxylated modified ZnO. *Sci. Rep.* **5**(1), 8968 (2015)
 106. Y.-L. Shi, F. Liang, Y. Hu, M.-P. Zhuo, X.-D. Wang, L.-S. Liao, High performance blue quantum dot light-emitting diodes employing polyethyleneimine ethoxylated as the interfacial modifier. *Nanoscale* **9**(39), 14792–14797 (2017)
 107. D. Li, J. Bai, T. Zhang, C. Chang, X. Jin, Z. Huang, B. Xu, Q. Li, Blue quantum dot light-emitting diodes with high luminance by improving the charge transfer balance. *Chem. Commun.* **55**(24), 3501–3504 (2019)
 108. X. Qu, J. Ma, S. Jia, Z. Wu, P. Liu, K. Wang, X.-W. Sun, Improved blue quantum dot light-emitting diodes via chlorine passivated ZnO nanoparticle layer. *Chin. Phys. B* **30**(11), 118503 (2021)
 109. T. Cheng, F. Wang, W. Sun, Z. Wang, J. Zhang, B. You, Y. Li, T. Hayat, A. Alsaedi, Tan, Z., High-performance blue quantum dot light-emitting diodes with balanced charge injection. *Adv. Elect. Mater.* **5**(4), 1800794 (2019)
 110. J.-H. Lee, C.-H. Chen, P.-H. Lee, H.-Y. Lin, M.-K. Leung, T.-L. Chiu, C.-F. Lin, Blue organic light-emitting diodes: current status, challenges, and future outlook. *J. Mater. Chem. C* **7**(20), 5874–5888 (2019)
 111. X. Xu, M.S. Weaver, J.J. Brown, In 61.2: phosphorescent stacked OLEDs for warm white lighting applications. *SID Symp. Dig. Tech. Pap.* **44**, 845–847 (2013)
 112. P. Wellmann, M. Hofmann, O. Zeika, A. Werner, J. Birnstock, R. Meerheim, G. He, K. Walzer, M. Pfeiffer, K. Leo, High-efficiency p-i-n organic light-emitting diodes with long lifetime. *J. SoC. Inf. Displ.* **13**(5), 393–397 (2005)
 113. R. Fan, X. Zhang, Z. Tu, Influence of ambient temperature on OLED lifetime and uniformity based on modified equivalent lifetime detection. *J. SoC. Inf. Displ.* **27**(10), 597–607 (2019)
 114. Y. Zou, J. Hu, M. Yu, J. Miao, Z. Xie, Y. Qiu, X. Cao, C. Yang, High-performance narrowband pure-red OLEDs with external quantum efficiencies up to 36.1% and ultralow efficiency roll-off. *Adv. Mater.* **34**(29), 2201442 (2022)
 115. S. Scholz, D. Kondakov, B. Lüssem, K. Leo, Degradation mechanisms and reactions in organic light-emitting devices. *Chem. Rev.* **115**(16), 8449–8503 (2015)
 116. Q. Khan, A. Subramanian, I. Ahmed, M. Khan, A. Nathan, G. Wang, L. Wei, J. Chen, Y. Zhang, Q. Bao, Overcoming the

- electroluminescence efficiency limitations in quantum-dot light-emitting diodes. *Adv. Opt. Mater.* **7**(20), 1900695 (2019)
117. I. Siddiqui, S. Kumar, Y.-F. Tsai, P. Gautam, K.K. Shahnawaz, J.-T. Lin, L. Khai, K.-H. Chou, A. Choudhury, S. Grigalevicius, J.-H. Jou, Status and challenges of blue OLEDs: a review. *Nanomaterials* **13**(18), 2521 (2023)
118. H. Shen, Q. Lin, W. Cao, C. Yang, N.T. Shewmon, H. Wang, J. Niu, L.S. Li, J. Xue, Efficient and long-lifetime full-color light-emitting diodes using high luminescence quantum yield thick-shell quantum dots. *Nanoscale* **9**(36), 13583–13591 (2017)
119. H. Shen, Q. Gao, Y. Zhang, Y. Lin, Q. Lin, Z. Li, L. Chen, Z. Zeng, X. Li, Y. Jia, Visible quantum dot light-emitting diodes with simultaneous high brightness and efficiency. *Nat. Photon* **13**(3), 192–197 (2019)
120. M. Gao, Y. Tu, D. Tian, H. Yang, X. Fang, F. Zhang, H. Shen, Z. Du, Alleviating electron over-injection for efficient cadmium-free quantum dot light-emitting diodes toward deep-blue emission. *ACS Photonics* **9**(4), 1400–1408 (2022)
121. J. Pan, J. Chen, Q. Huang, L. Wang, W. Lei, A highly efficient quantum dot light emitting diode via improving the carrier balance by modulating the hole transport. *RSC Adv.* **7**(69), 43366–43372 (2017)
122. X. Hou, J. Kang, H. Qin, X. Chen, J. Ma, J. Zhou, L. Chen, L. Wang, L.-W. Wang, X. Peng, Engineering Auger recombination in colloidal quantum dots via dielectric screening. *Nat. Commun.* **10**(1), 1750 (2019)
123. D.S. Chung, T. Davidson-Hall, G. Cotella, Q. Lyu, P. Chun, H. Aziz, Significant lifetime enhancement in QLEDs by reducing interfacial charge accumulation via fluorine incorporation in the ZnO electron transport layer. *Nano-Micro Letts.* **14**(1), 212 (2022)
124. S. Chen, W. Cao, T. Liu, S.-W. Tsang, Y. Yang, X. Yan, L. Qian, On the degradation mechanisms of quantum-dot light-emitting diodes. *Nat. Commun.* **10**(1), 765 (2019)

Publisher's Note Springer Nature remains neutral with regard to jurisdictional claims in published maps and institutional affiliations.

Springer Nature or its licensor (e.g. a society or other partner) holds exclusive rights to this article under a publishing agreement with the author(s) or other rightsholder(s); author self-archiving of the accepted manuscript version of this article is solely governed by the terms of such publishing agreement and applicable law.